NOTICE

CERTAIN DATA CONTAINED IN THIS DOCUMENT MAY BE DIFFICULT TO READ IN MICROFICHE PRODUCTS.

CHARACTERIZATION OF FLOW IN FRACTURED TUFF USING COMPUTERIZED TOMOGRAPHY

LA-SUB--93-83

DE93 008910

Prepared By:

Conrad W. Felice
and
John C. Sharer

Submitted to

University of California
Los Alamos National Laboratory
P. O. Box 990
Los Alamos, New Mexico 87545

Attn: Dr. Everett P. Springer

Submitted by:

TerraTek, Inc.
University Research Park
400 Wakara Way
Salt Lake City, Utah 84108

TR92-27
September 1991

Table of Contents

List of Tables

List of Figures

1.0 INTRODUCTION

1.1 Objective

The objective of this effort was to demonstrate TerraTek's capability to use X-ray computerized tomography (CT) to observe fluid flow down a fracture and rock matrix imbibition in a sample of Bandelier tuff.

To accomplish the objective, a tuff sample 152.4 mm long and 50.8 mm in diameter was prepared. A portion of the sample was artificially fractured and coupled to a section of matrix material so that the fracture was not exposed. Water was flowed through the sample at five flow rates and CT scanning performed at set intervals during the flow. Cross sectional images and longitudinal reconstructions were built and saturation profiles calculated for the sample at each time interval at each flow rate. The results showed that for the test conditions, the fracture was not a primary pathway of fluid flow down the sample. Fluid flow was governed by the high imbibition capability of the rock matrix material.

1.2 Background

At hazardous waste sites, information on contaminant flow and transport characteristics in the specific geologic setting are needed to successfully design and implement remediation systems. At fractured rock sites, geologic and hydrogeologic properties of the system are difficult to collect, hence designs have been based on theoretical analysis. However, theoretical analysis alone is not sufficient. Analyses based on mathematical models require the necessary data for reliable and valid predictions of the rate and direction of groundwater flow and contaminate transport. Decision makers must feel confident that the model selected provides information relevant to the system of conditions to which it is applied. Hence, validation is a necessary component in the development process of any predictive mathematical model.

X-ray CT is a nondestructive testing technique that can provide a firm basis for understanding the phenomena associated with contaminant transport and flow in fractured rock under controlled conditions. The objective of this effort was to use X-ray CT to observe the flow of water through a rock core containing a single fracture. Because of the sensitivity of the method to effective atomic number, it is possible to detect variations in pore fluid composition. Fluids containing elements of higher atomic number, such as Chlorine, Iodine, or heavy metals, are

easily distinguished from water or light hydrocarbons. Even gas phases can be traced by using heavy inert gases like Xenon. These differences can be calibrated in order to determine relative saturation levels of each phase in three dimensions. The progress of each phase through the sample can be observed in real time without the need for collecting and analyzing effluent samples.

2.0 SAMPLE PREPARATION AND TEST PROCEDURES

2.1 Samples

The Los Alamos National Laboratory provided TerraTek with samples of Bandelier tuff. The samples were cylindrical core approximately 50.8 mm (2.0 in) in diameter and of varying lengths. The samples were shipped in a wooden crate with each sample resting in a styrofoam cradle. Paper padding was placed around the samples. The samples were not preserved, and appeared dry and very fragile. Table 1 is a partial reproduction of the log shipped with the samples.

Table 1: Sample Log.

Box #	Interval (ft)	Useable Length (in)	Estimated Diameter (in)	Individual Sample Conditions	
1	49-59	8	2	Top	1 pc
1	49-59	3 & 5	2		2 pc
1	49-59	<1 & 6	2		2 pc
1	49-59	2 & 5	2	Bottom	2 pc
1	59-69	5	2	Top	1 pc
1	59-69	6	2		1 pc
1	59-69	6.5	2		1 pc
1	59-69	7	2	Bottom	1 pc

Lithologically, the material is a crystal-vitric tuff (borderline crystal-lithic tuff) massive, very poorly sorted, and poorly indurated. No indication of grading or of being reworked was observed. The samples contained no fractures. The samples consisted of approximately 42.5% light brownish gray groundmass, 42% phenocrysts, 8% light bluish gray lithics and 7.5% light gray pumice fragments. The groundmass consisted of fine grained ash which has an unaltered

appearance. Phenocrysts consist of approximately 20% euhedral to subhedral quartz with an average size of 2.0 mm, 20% euhedral to subhedral feldspars with an average size of 1.75 mm, and about 1% each of subhedral biotite and hornblende with an average size of .75 mm and 1.0 mm, respectively. Lithic fragments are subangular to subrounded and range from 0.5 mm to 10 mm with an average size of 1.5 mm. Pumice fragments appear angular and range from 1 mm to 10 mm in length and average 3 mm. Pumice fragments are predominately vesicular exhibiting minor (if any) evidence of devitrification.

A core from interval 49 ft to 59 ft was selected for testing. To aid in sample preparation, the selected piece of core was coated with epoxy (Figure 1). As shown in Figure 1, the epoxy did not penetrate the tuff. The sample was cut with a wire saw to the specified length of 152.4 mm (6.0 in).

Figure 1: Epoxy Coated Sample.

Because the sample did not contain a natural fracture, an artificial one was created. This was done by cutting the core in half down its length with the wire saw (Figure 2). Before creating the artificial fracture, a 38.1 mm (1.5 in) [illegible] section was cut from one end of the sample. For testing, this end section was placed against the fractured section with a piece of filter paper

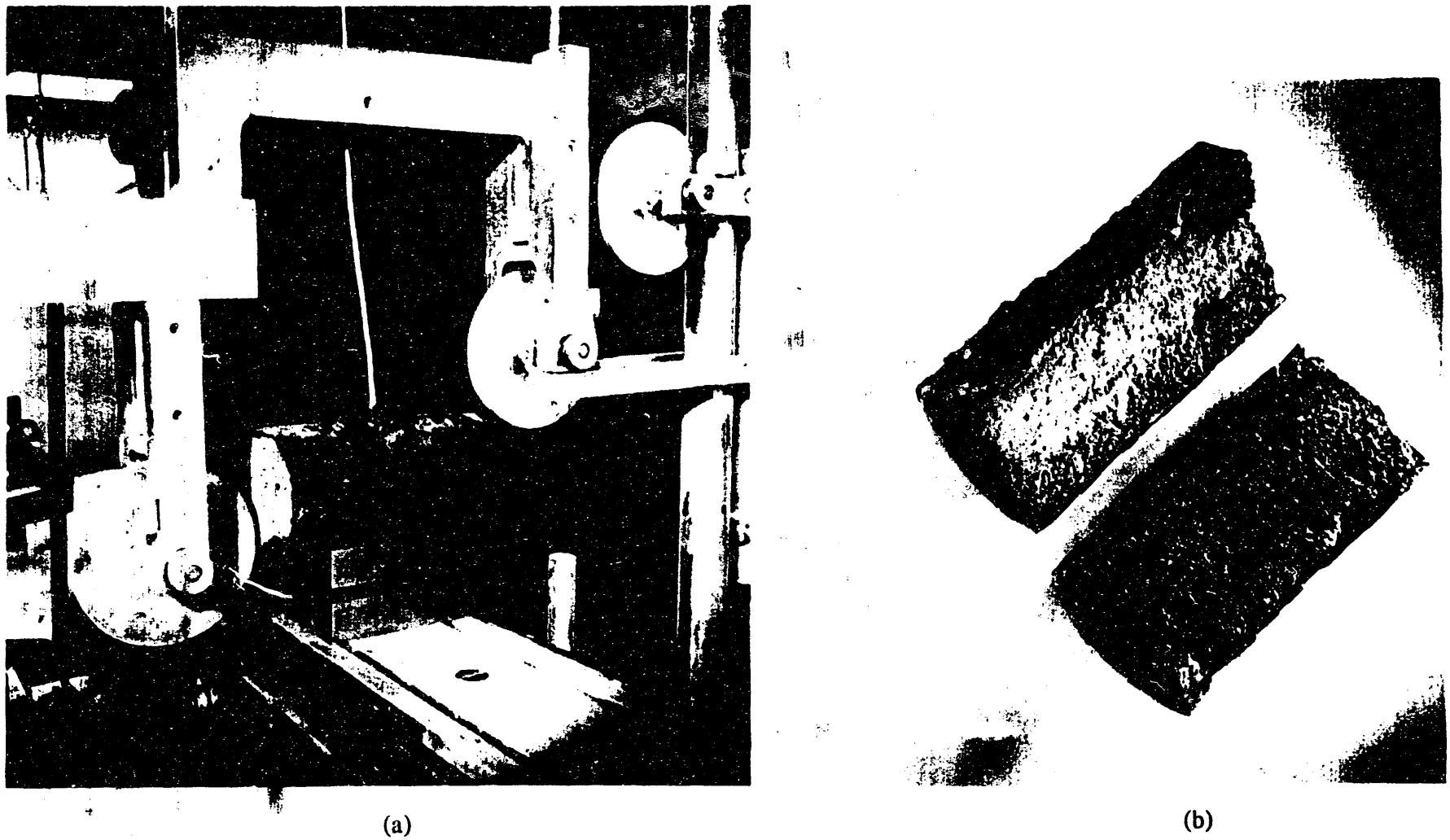

(a) (b)

Figure 2: a) Creating artificial fracture with wiresaw, b) cut surface.

between the two sections. This end section of matrix material effectively terminated the fracture so that it was not exposed. Figure 3 shows the final sample dimensions.

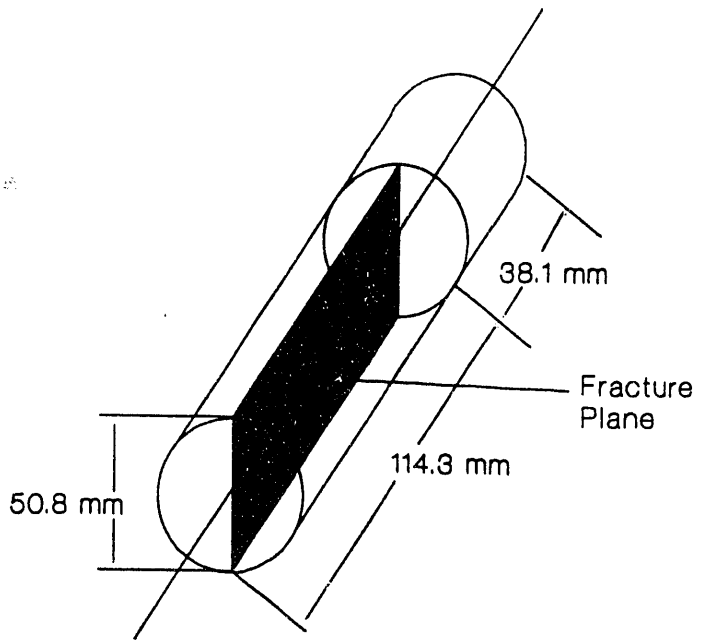

Figure 3: Sample Dimensions.

2.2 *Test procedures*

The sample was jacketed in a rubber sleeve and placed in an aluminum pressure vessel. The vessel was then placed in the CT scanning unit. Appendix A includes a description of the terminology, test equipment, and analysis procedures.

A 2 MPa (300 psi) hydrostatic pressure was applied to the sample. Before beginning the flow of water, the sample was scanned to establish the initial test conditions. To compute the saturation profiles during the test, it was assumed that the initial conditions represented zero water saturation. The sample was scanned continuously with a beam thickness of 10 mm. With a sample length of 152.4 mm, 15 scans were needed to traverse the entire sample.

Five flow rates were selected: 0.1 cc/min, 0.4 cc/min, 1.0 cc/min, 2.0 cc/min, and 5.0 cc/min. To enhance image quality and ensure a significant variation in attenuation, the water was doped with 10% sodium iodide. The iodine has a high attenuation coefficient and provides significant contrast to accurately determine saturation profiles. Water flow was initiated over the full face of the sample at the specified rates. The fracture orientation was vertical. The flow conditions allowed the water to diffuse through the sample, retarded only by imbibition or other interactions with the fracture and rock matrix.

At the flow rate of 0.1 cc/min, the sample was completely scanned at 30 minute intervals. At each subsequent rate, the flow and saturation were allowed to equilibrate before the sample was scanned. The sample was assumed to be fully saturated after reaching equilibrium at the 5.0 cc/min flow rate. This condition coupled with the initial scan set were used to compute the saturation profiles. With two saturation levels and corresponding CT numbers, a linear

interpolation was performed to determine the degree of saturation for each location along the length of the sample.

3.0 RESULTS AND DISCUSSION

3.1 Results

Figures 4 and 5 show the cross sectional images and longitudinal reconstruction of the sample at the initial conditions under the hydrostatic pressure of 2 MPa (300 psi). The longitudinal reconstructions were taken perpendicular to the fracture plane as shown in Figure 6. Each set represents 15 scans or a complete traverse of the sample. Figures 7 to 25 are the longitudinal reconstructions and saturation profiles at the end of each set for each flow rate. Table 2 references the sets of scans performed at each flow rate.

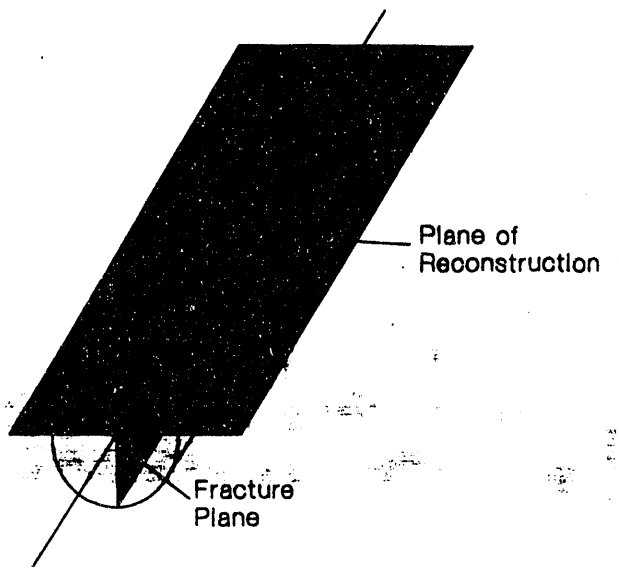

Figure 6: Orientation of Longitudinal reconstruction.

Cross sectional images are the illustrations depicting an individual CT scan. The images are plotted consecutively on the pages in a left to right and top to bottom order. The images are positioned in the order in which they were acquired. A six digit scan number (i.e., 100035) is printed directly below each image. Each cross sectional image is made up of a 256 x 256 array of data. The CT numbers are defined as normalized attenuation coefficients for the sample. The thickness of the X-ray beam determines the volume of material used in the calculation of the attenuation coefficient. Subsequently, colors are assigned to the CT numbers to highlight contrasts. Red is assigned to show a region with a higher degree of saturation and blue to regions with a lower degree of saturation. Variations from red to blue are shown in the color bars to the left of the images. A region of interest for each cross sectional image equal to about 80% of the area of each slice was defined and average CT numbers for that region computed. The saturation for each location along the sample length was determined from these data and the assumed end point saturation stated above.

Figure 4

Cross Sectional Images
of Sample at
Initial Conditions

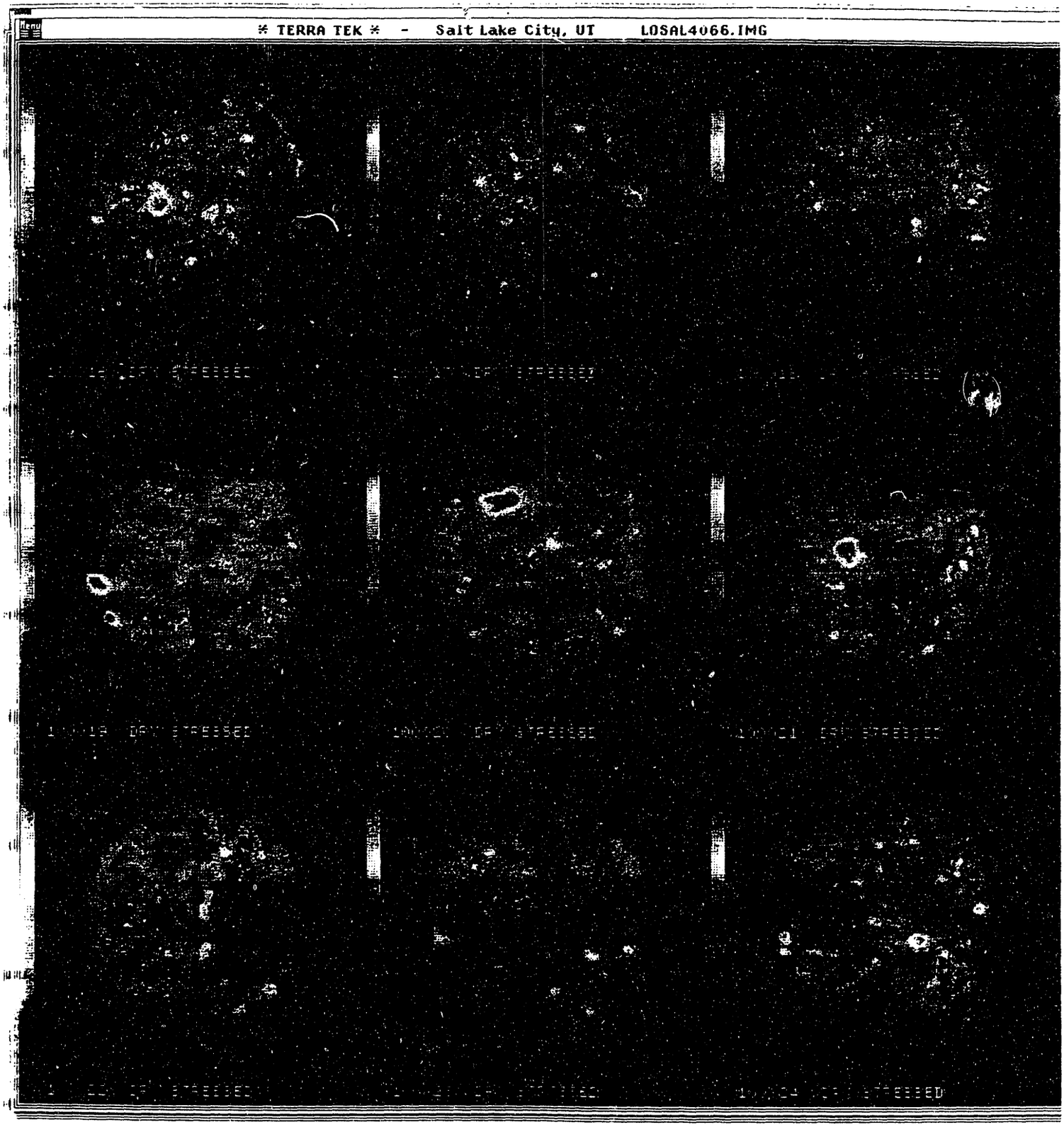

Figure 4
(Cont'd)

Cross-sectional Images
of Sample at
Initial Conditions

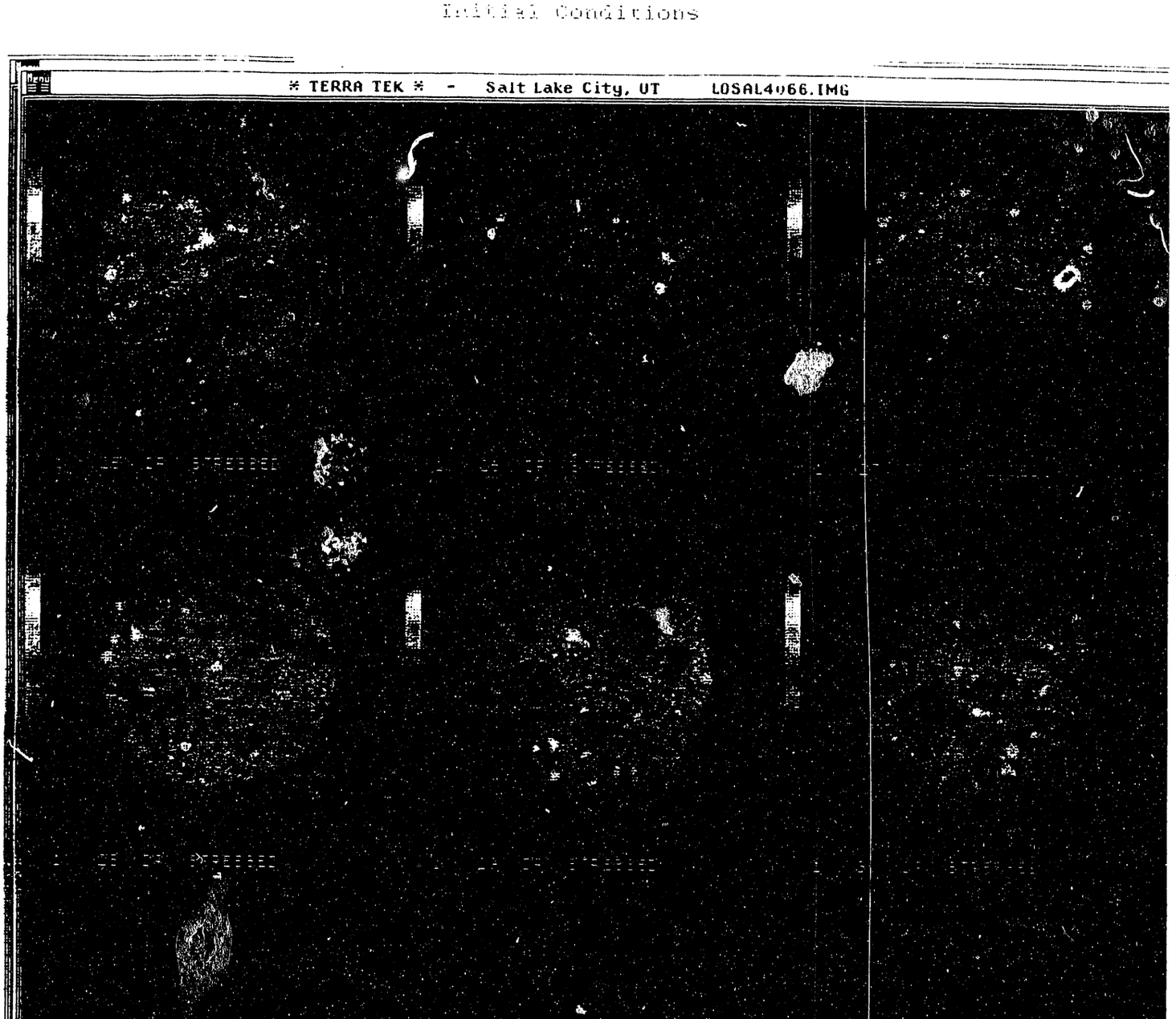

Figure 5

Longitudinal Reconstruction
at Initial Conditions

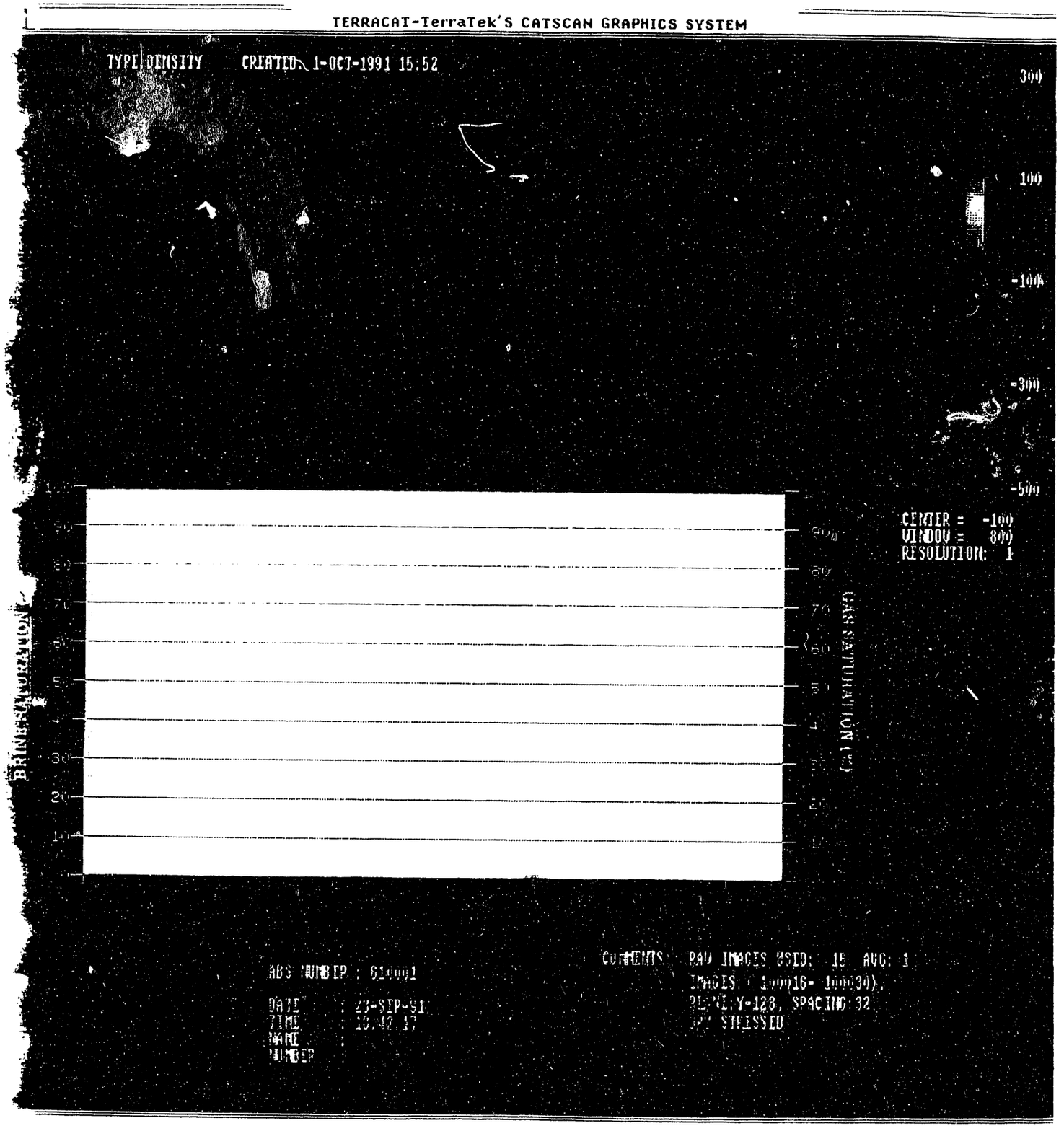

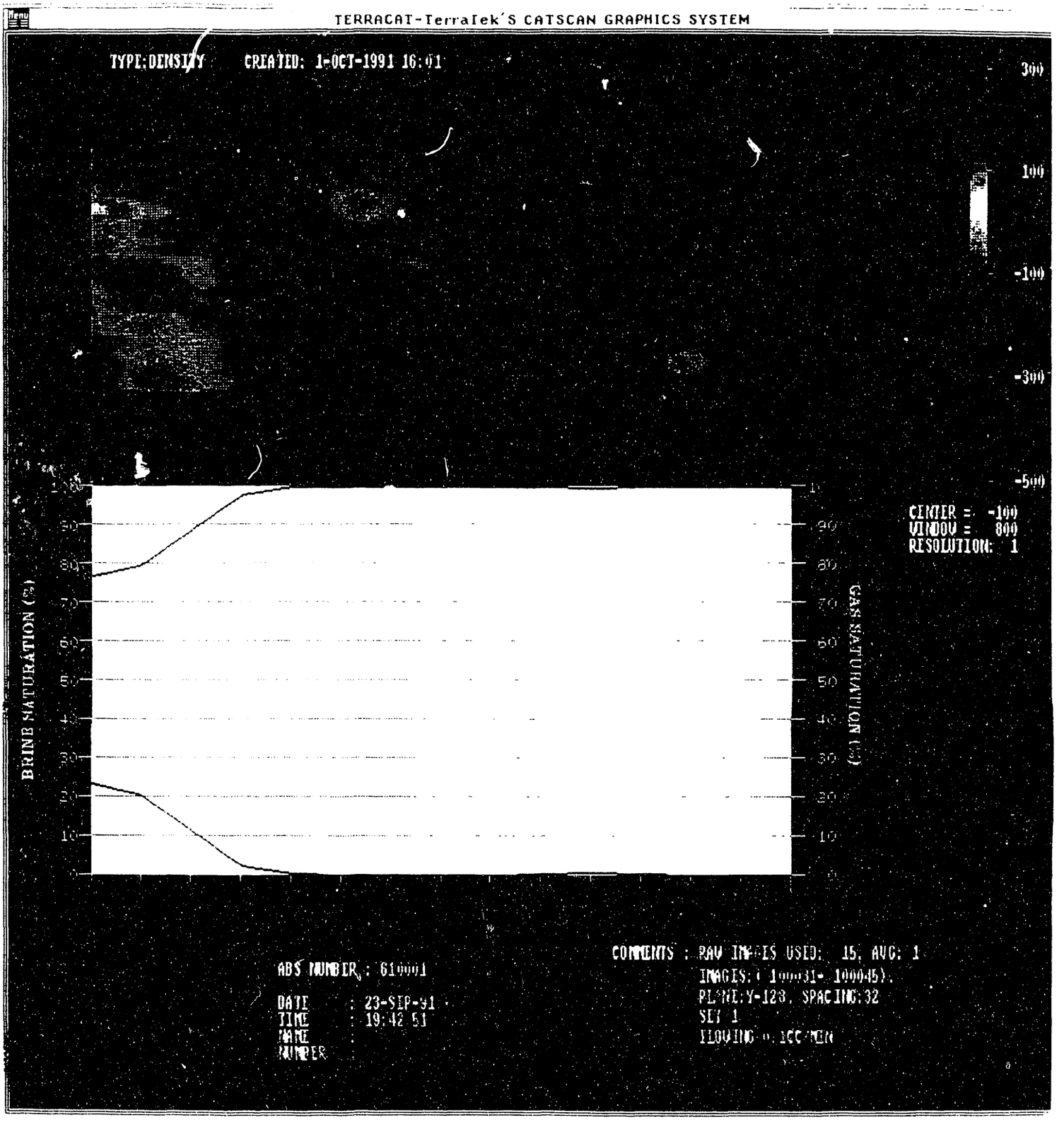
TERRACAT-TerraTek'S CATSCAN GRAPHICS SYSTEM
TYPE:DENSITY
CREATED: 1-OCT-1991 16:01
300
100
-100
-300
-500
CENTER = -100
WINDOW = 800
RESOLUTION: 1
BRINE SATURATION (%)
GAS SATURATION (%)
ABS NUMBER : 610001
DATE : 23-SEP-91
TIME : 19:42:51
NAME :
NUMBER :
COMMENTS : RAW IMAGES USED: 15, AVG: 1
IMAGES: (100031- 100045).
PLANE:Y-123, SPACING:32
SET 1
FLOWING 0.1CC/MIN

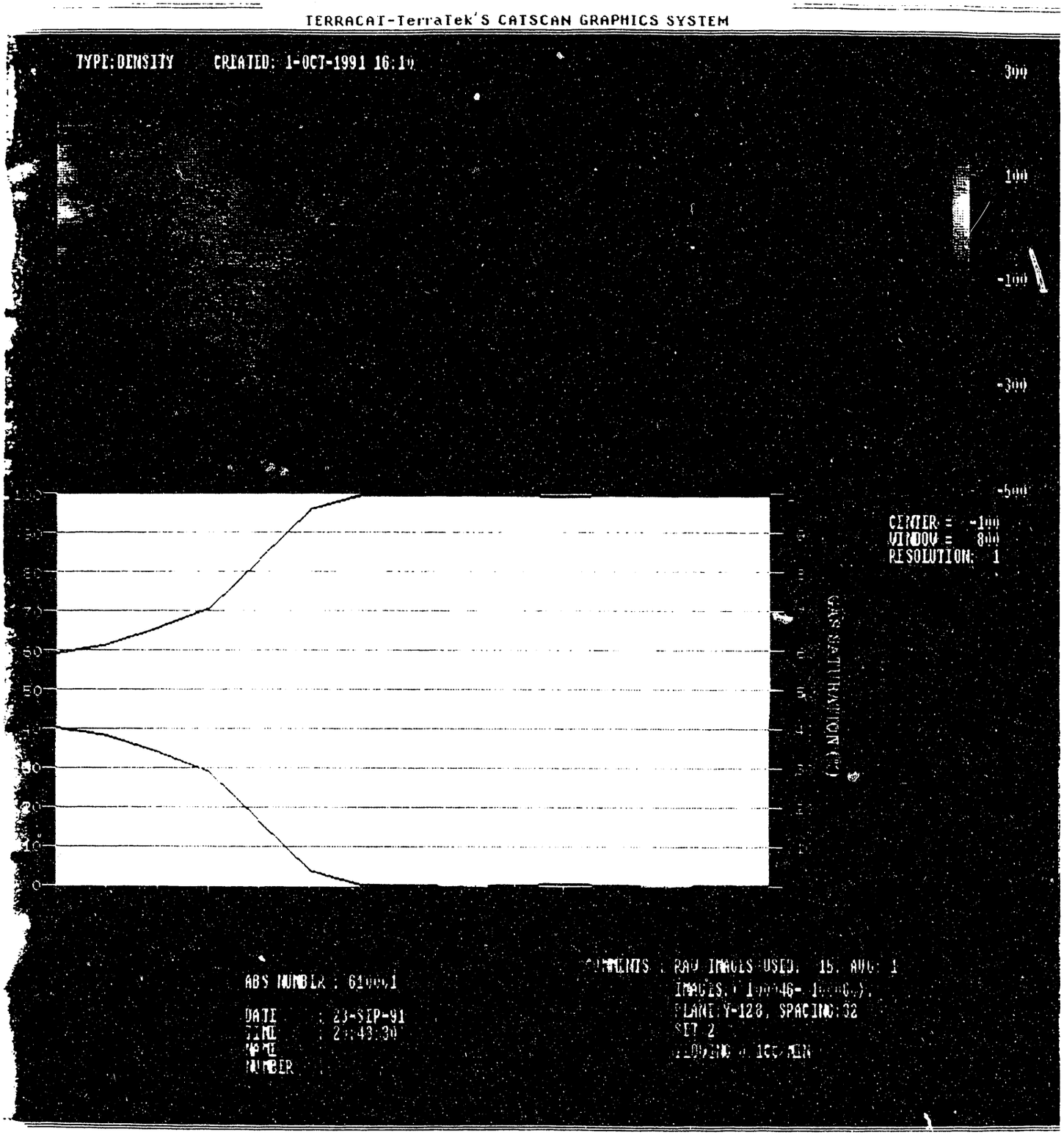
TERRACAT-TerraTek'S CATSCAN GRAPHICS SYSTEM
TYPE:DENSITY
CREATED: 1-OCT-1991 16:19
300
100
-100
-300
-500
CENTER = -100
WIDOW = 800
RESOLUTION: 1
GAS SATURATION (%)
ABS NUMBER : 61000.1
DATE : 23-SEP-91
TIME : 21:43:30
RAW IMAGES USED: 15, AVG: 1
SET 2

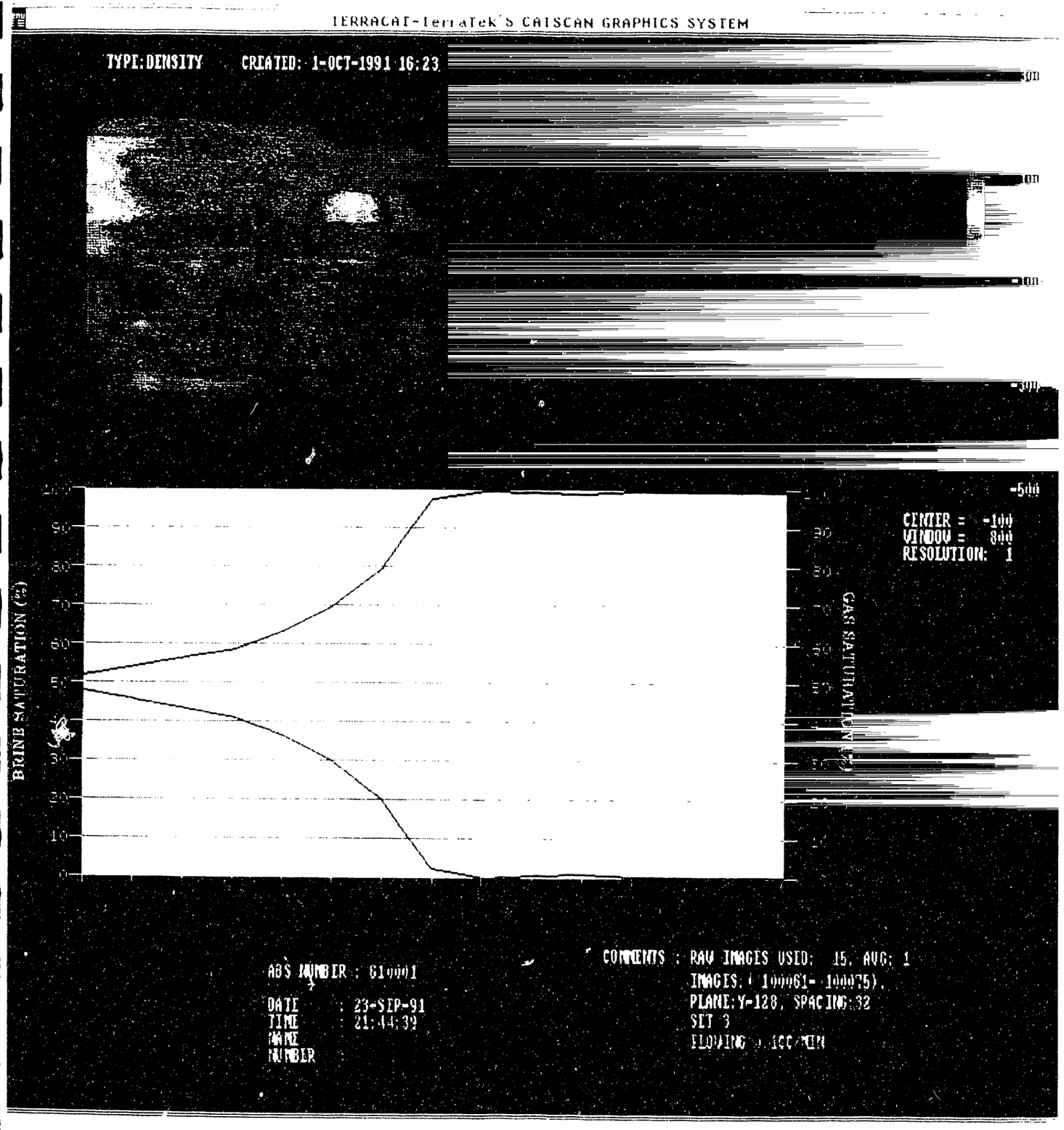
TERRACAT-TerraTek's CATSCAN GRAPHICS SYSTEM
TYPE:DENSITY
CREATED: 1-OCT-1991 16:23
CENTER = -100
WINDOW = 800
RESOLUTION: 1
BRINE SATURATION (%)
GAS SATURATION (%)
ABS NUMBER : 610001
DATE : 23-SEP-91
TIME : 21:44:39
COMMENTS : RAW IMAGES USED: 15, AVG: 1
IMAGES: (100061- 100075),
PLANE:Y-128, SPACING:32
SET 3

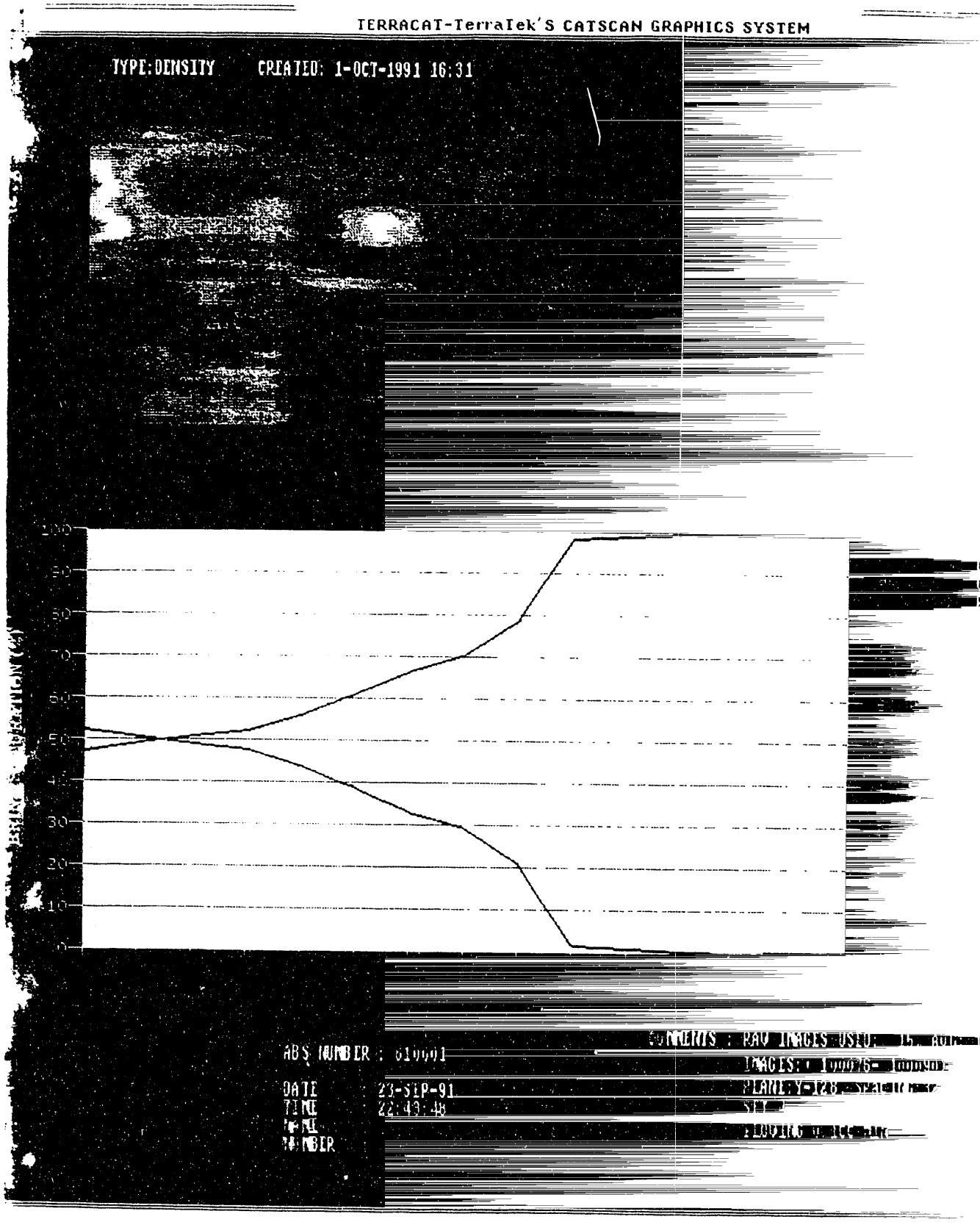
TERRACAT-TerraTek'S CATSCAN GRAPHICS SYSTEM
TYPE:DENSITY
CREATED: 1-OCT-1991 16:31
100
90
80
70
60
50
40
30
20
10
0
ABS NUMBER : 010001
DATE 23-SEP-91
TIME 22:49:48

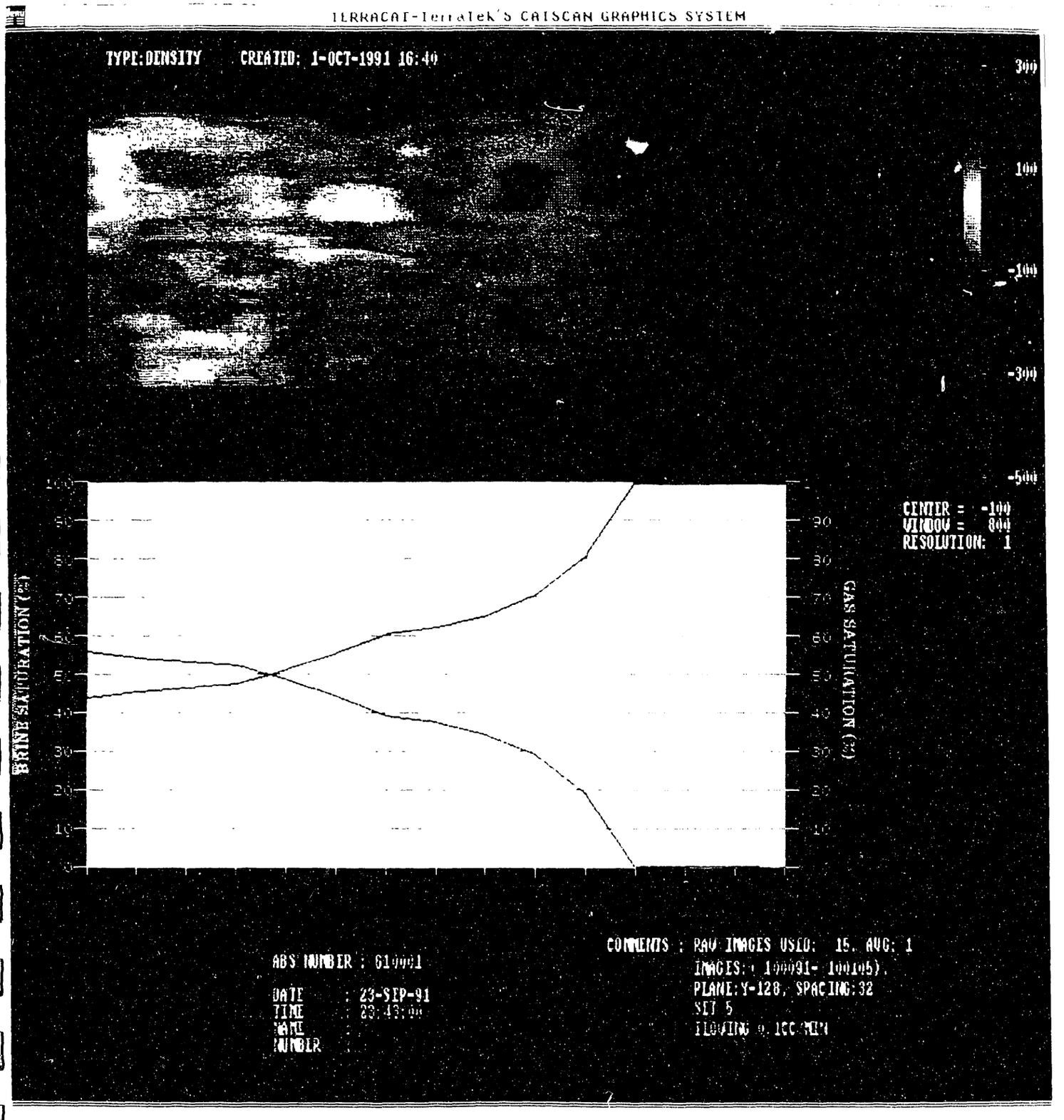
TERRACAT-TerraTek'S CATSCAN GRAPHICS SYSTEM
TYPE:DENSITY
CREATED: 1-OCT-1991 16:40
300
100
-100
-300
-500
CENTER = -100
WINDOW = 800
RESOLUTION: 1
BRINE SATURATION (%)
GAS SATURATION (%)
ABS NUMBER : 610001
DATE : 23-SEP-91
TIME : 23:43:00
NAME :
NUMBER :
COMMENTS : RAW IMAGES USED: 15, AVG: 1
IMAGES: (100091- 100105).
PLANE:Y-128, SPACING:32
SET 5
FLOWING 0.100 CC/MIN

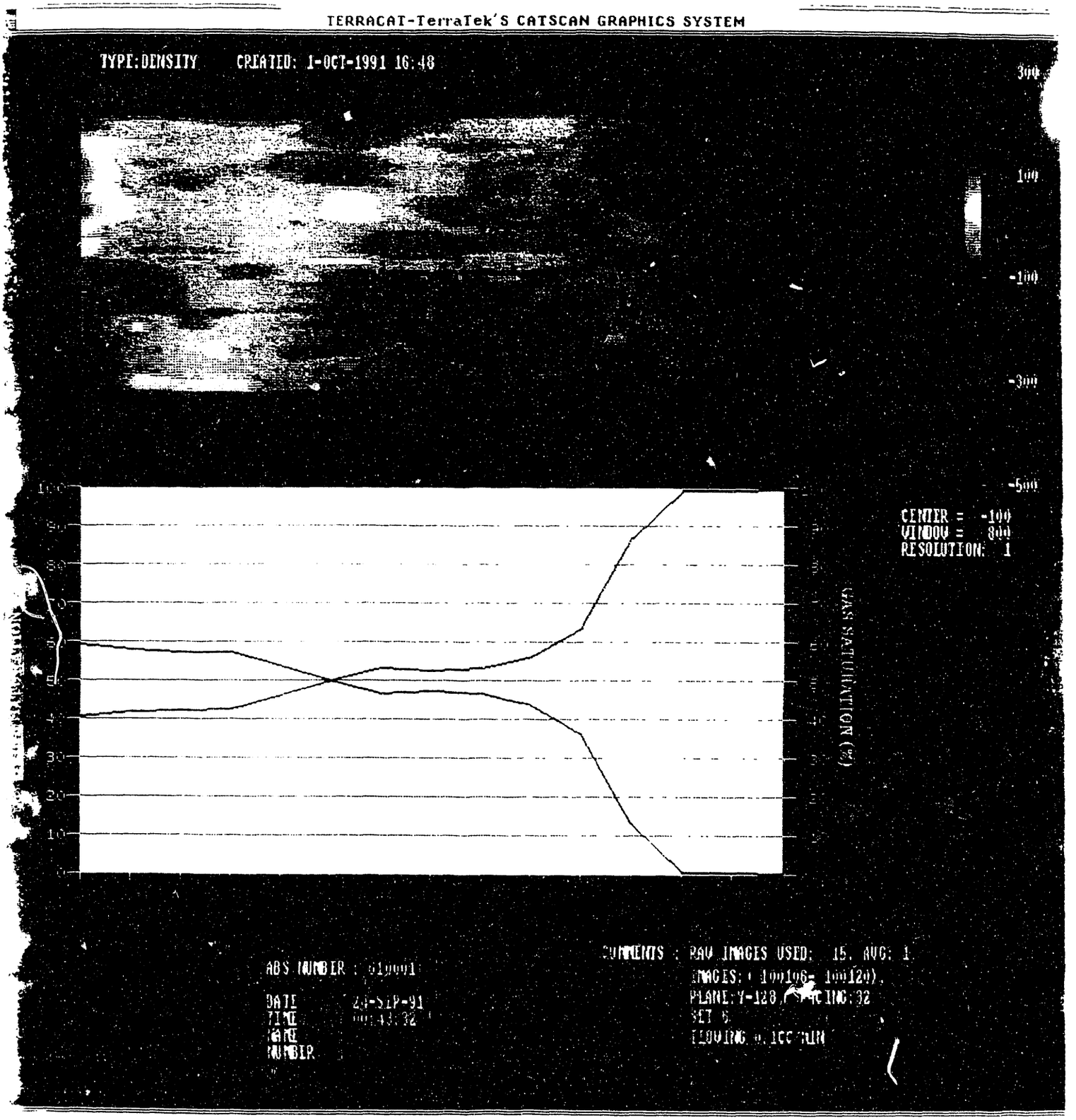
TERRACAT-TerraTek'S CATSCAN GRAPHICS SYSTEM
TYPE:DENSITY
CREATED: 1-OCT-1991 16:48
300
100
-100
-300
-500
CENTER = -100
WINDOW = 800
RESOLUTION: 1
(%) SATURATION
ABS NUMBER : 01001
DATE 24-SEP-91
TIME 00:43:32
SCAN NUMBER
COMMENTS : RAW IMAGES USED: 15, AVG: 1
IMAGES: (100106- 100120),
PLANE: Y-128 (SCANNING:32
SET 6
FLOWING 0.100 GUM

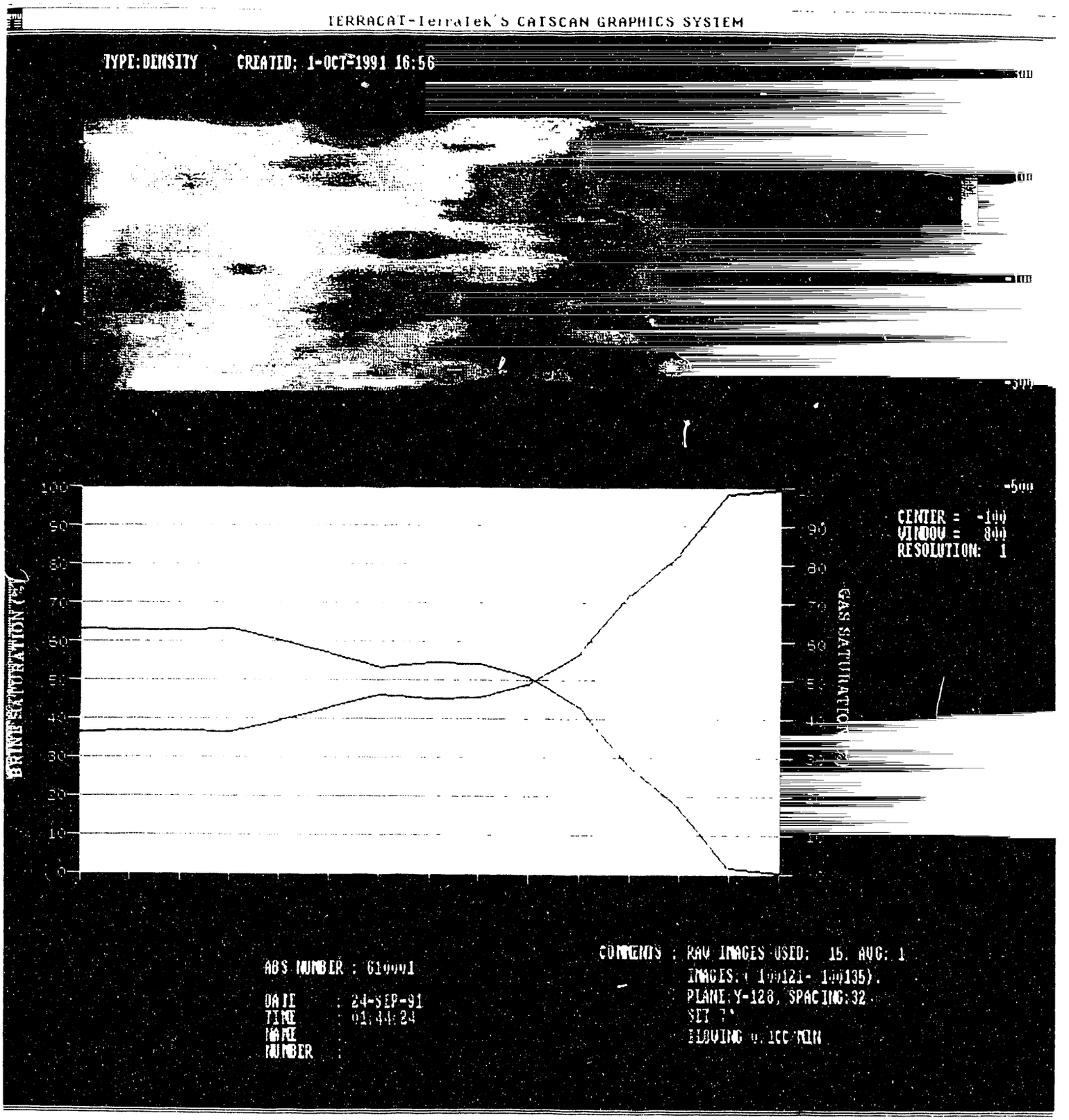
TERRACAT-Terratek's CATSCAN GRAPHICS SYSTEM
TYPE:DENSITY
CREATED: 1-OCT-1991 16:56
-500
-500
CENTER = -100
WINDOW = 800
RESOLUTION: 1
BRINE SATURATION (%)
GAS SATURATION
100
90
80
70
60
50
40
30
20
10
0
ABS NUMBER : 610001
DATE : 24-SEP-91
TIME : 01:44:24
NAME
NUMBER :
COMMENTS : RAW IMAGES USED: 15. AVG: 1
IMAGES: (100121- 100135).
PLANE:Y-128, SPACING:32.
SET ?*
FLOWING 0.1CC/MIN

Figure 14: Typical

Longitudinal Reconstruction
With Saturation Profile
At 0.1 cm/min.

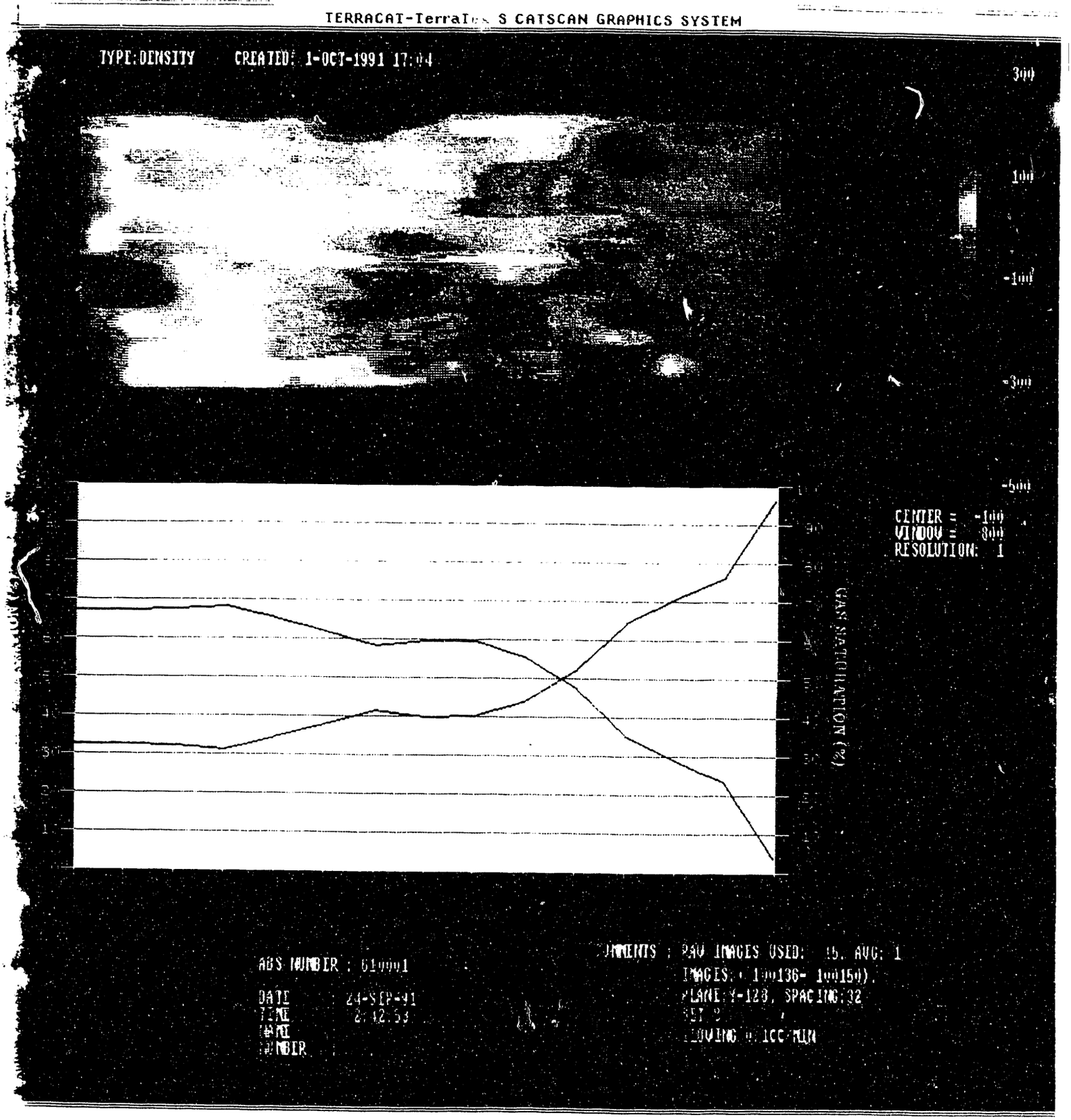

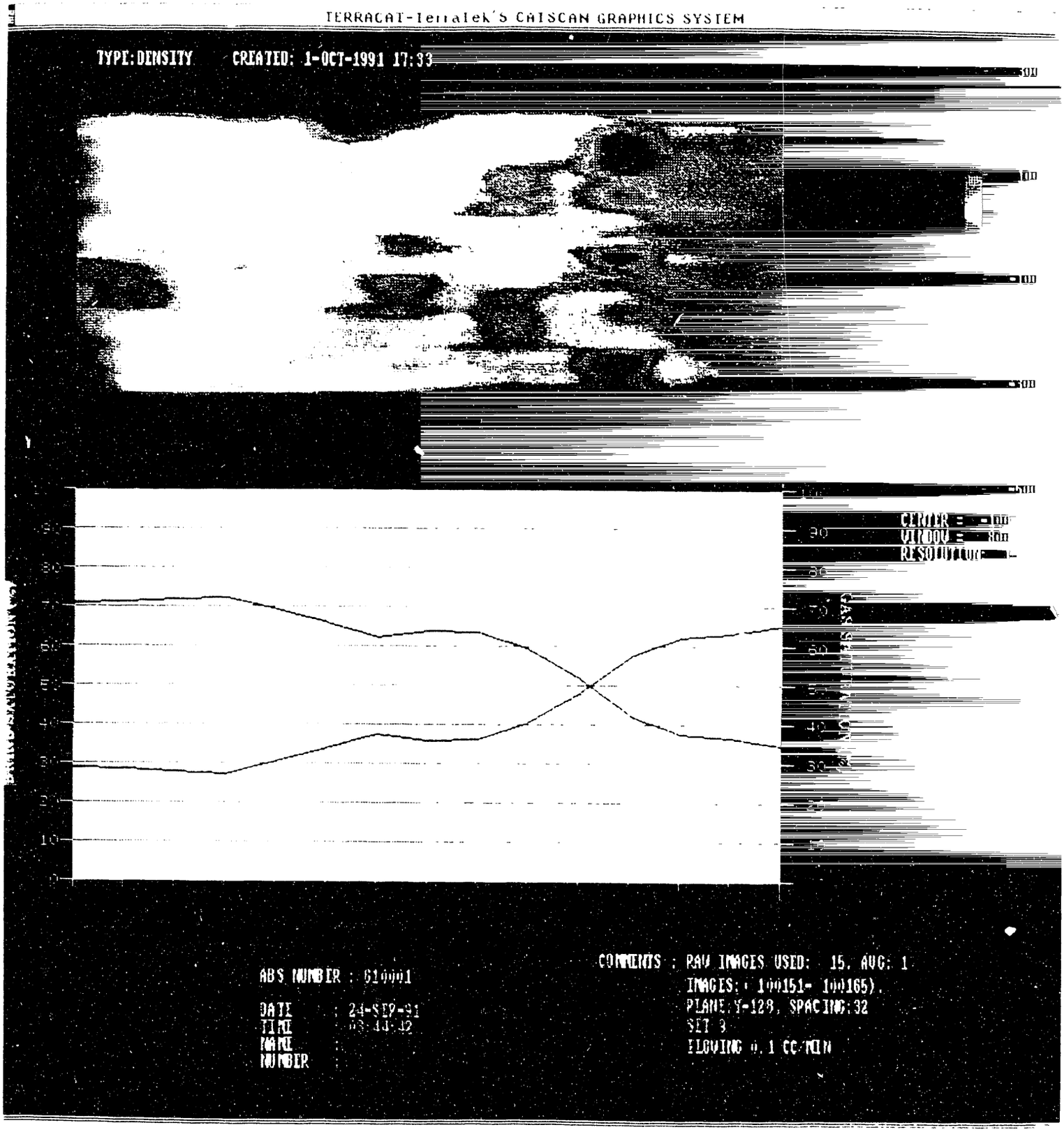
TERRACAT-Terratek's CATSCAN GRAPHICS SYSTEM
TYPE:DENSITY
CREATED: 1-OCT-1991 17:33
CENTER
VIEWOW
RESOLUTION
GAS SATURATION
ABS NUMBER : 610001
DATE : 24-SEP-91
TIME : 03:44:42
NAME :
NUMBER :
COMMENTS : RAW IMAGES USED: 15, AVG: 1
IMAGES: (100151- 100165).
PLANE:Y-128, SPACING:32
SET 3
FLOWING 0.1 CC/MIN

Longitudinal Permeability
with Saturation Flooding
at 0.1 cc/min.

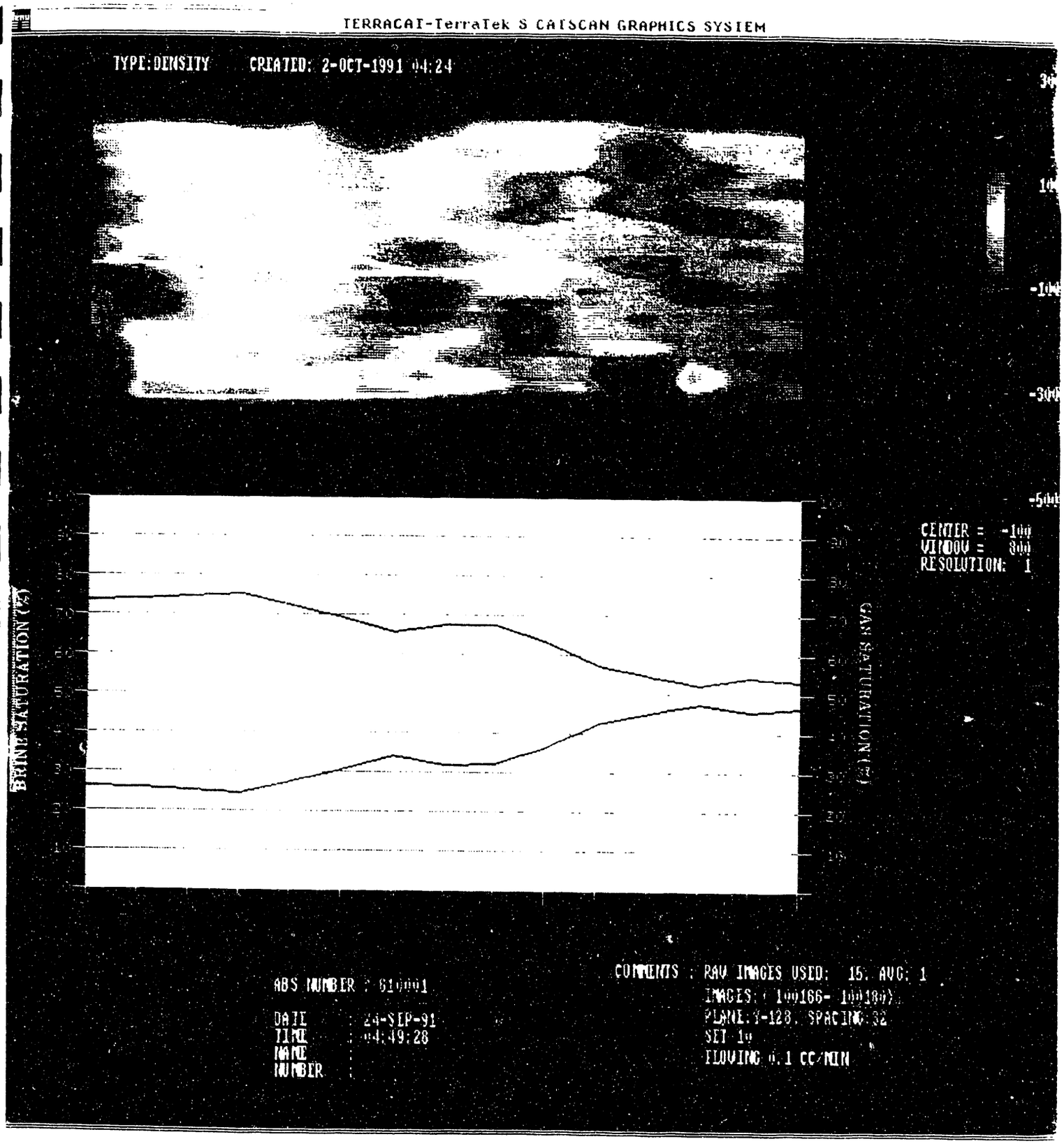

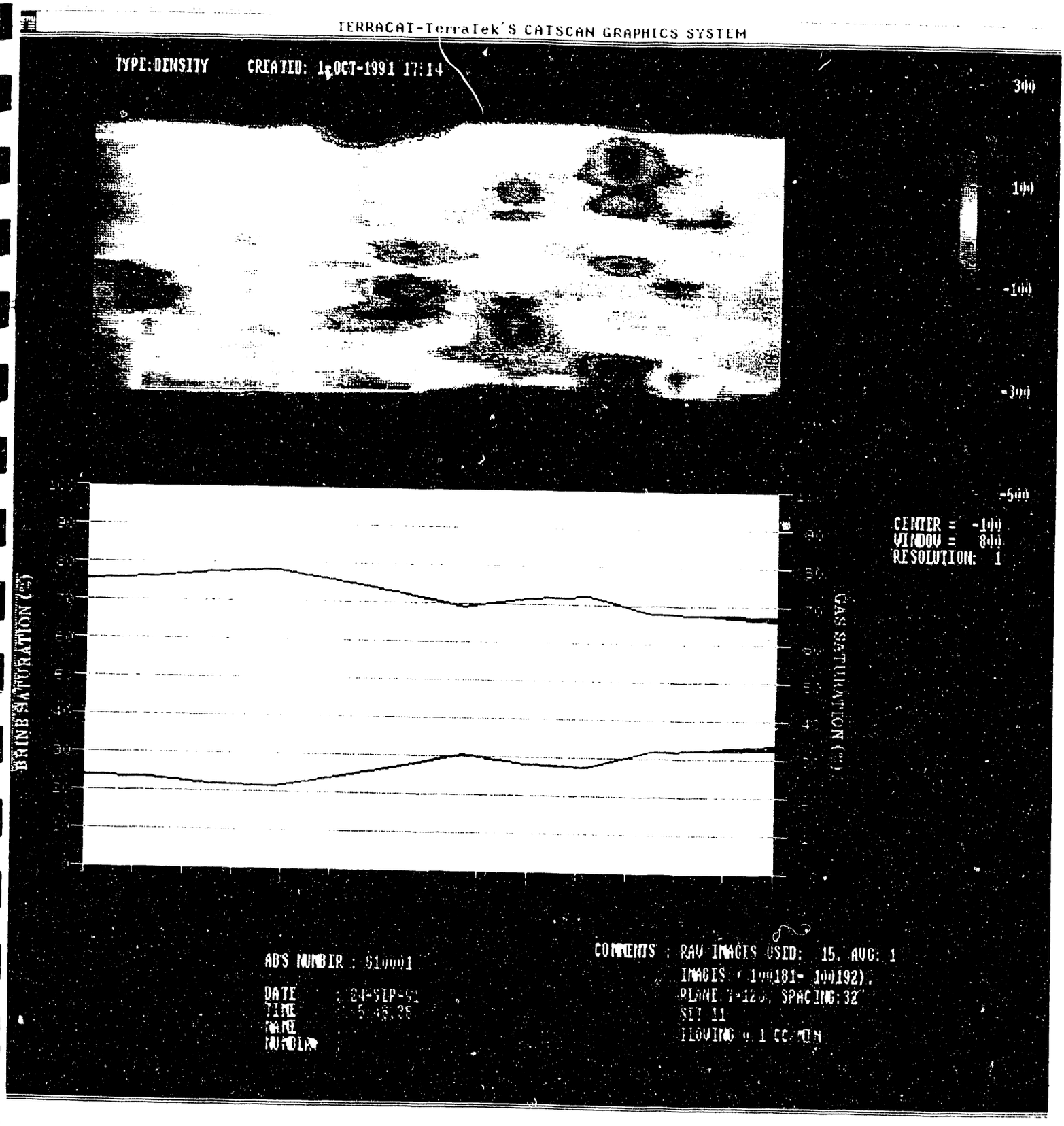
TERRACAT-TerraTek'S CATSCAN GRAPHICS SYSTEM
TYPE:DENSITY
CREATED: 1-OCT-1991 17:14
300
100
-100
-300
-500
CENTER = -100
WINDOW = 800
RESOLUTION: 1
BRINE SATURATION (%)
GAS SATURATION (%)
ABS NUMBER : S10001
DATE : 24-SEP-91
TIME : 5:46.36
COMMENTS : RAW IMAGES USED: 15. AUG: 1
IMAGES (100181- 100192).
PLANE 7-12 , SPACING:32
SET 11
FLOWING @ 1 CC/MIN

Longitudinal Reconstruction
with Saturation Profile
at 0.1 cc min.

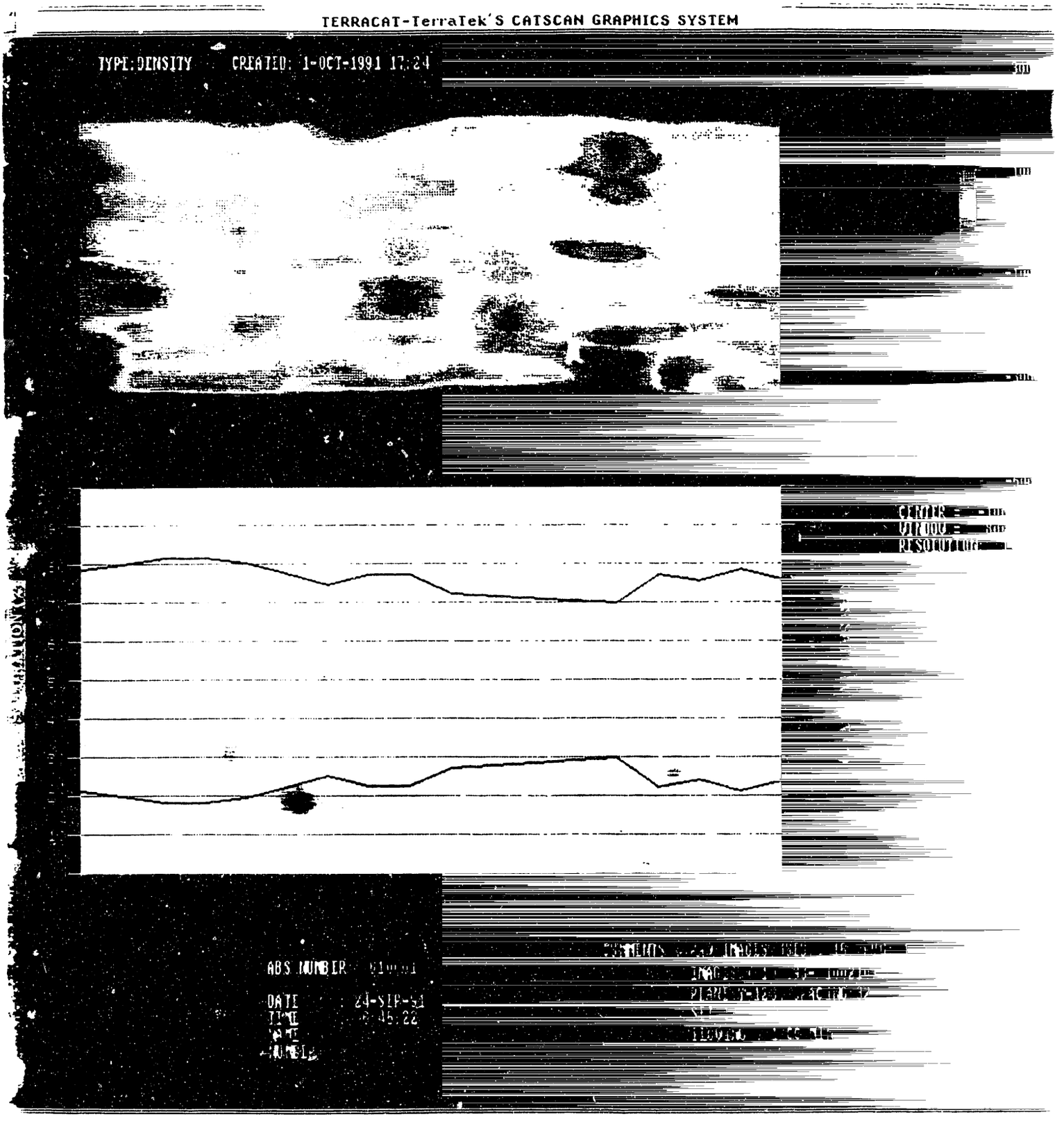

Longitudinal Reconstruction
with Saturation Profile
at 0.1 cc/min.

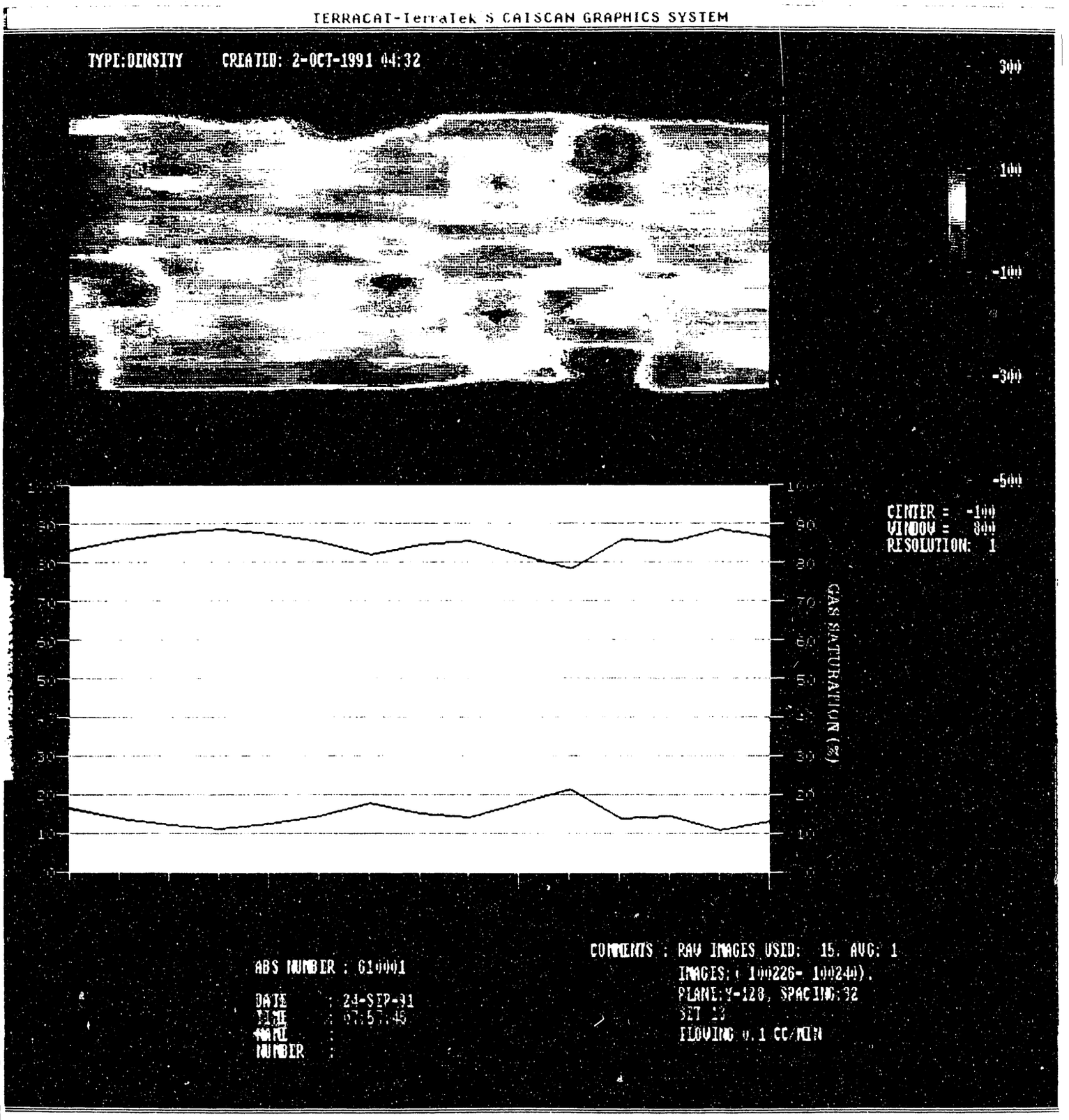

Longitudinal Reconstruction
with Saturation Profile
at 0.1 cc/min.

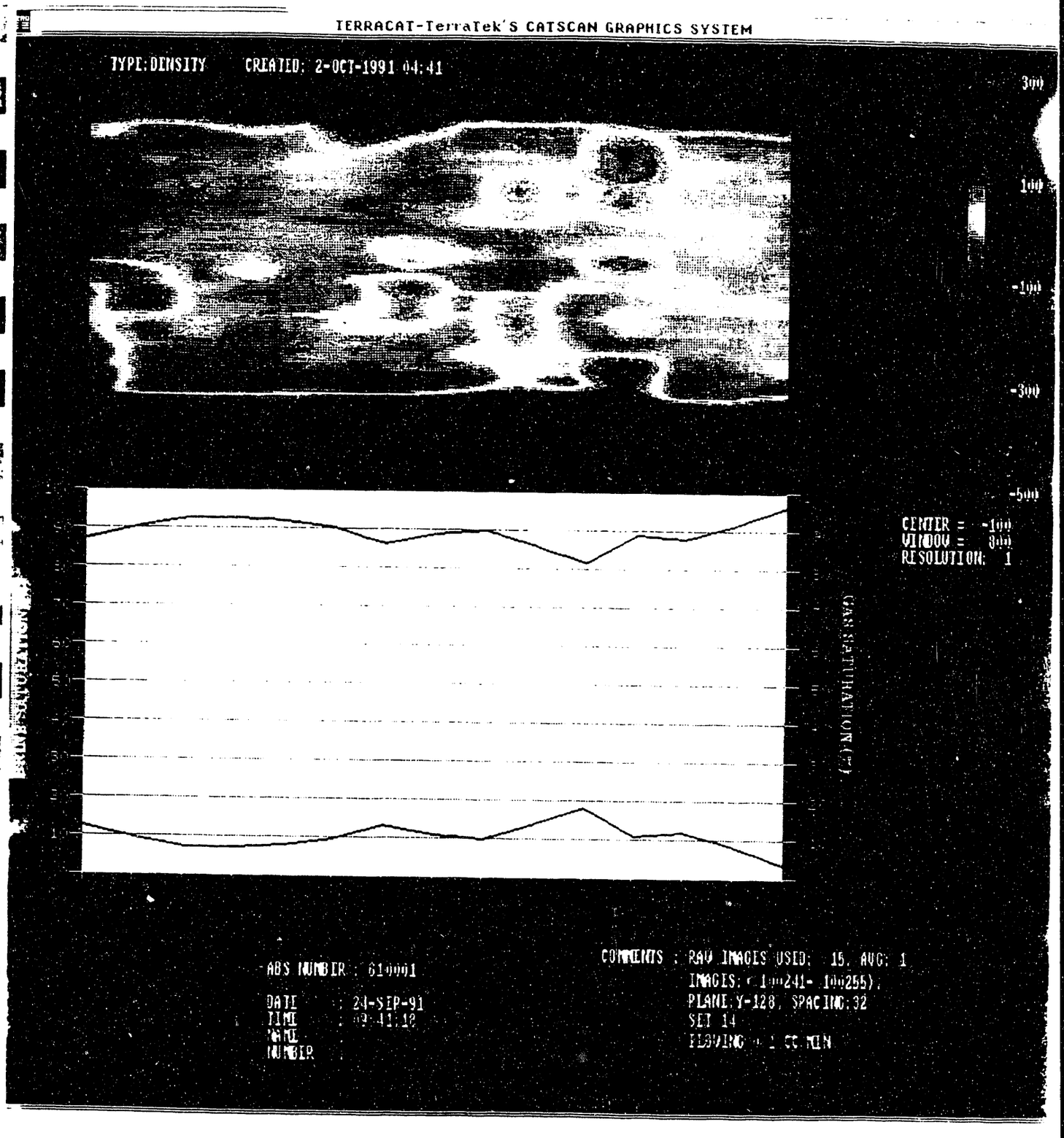

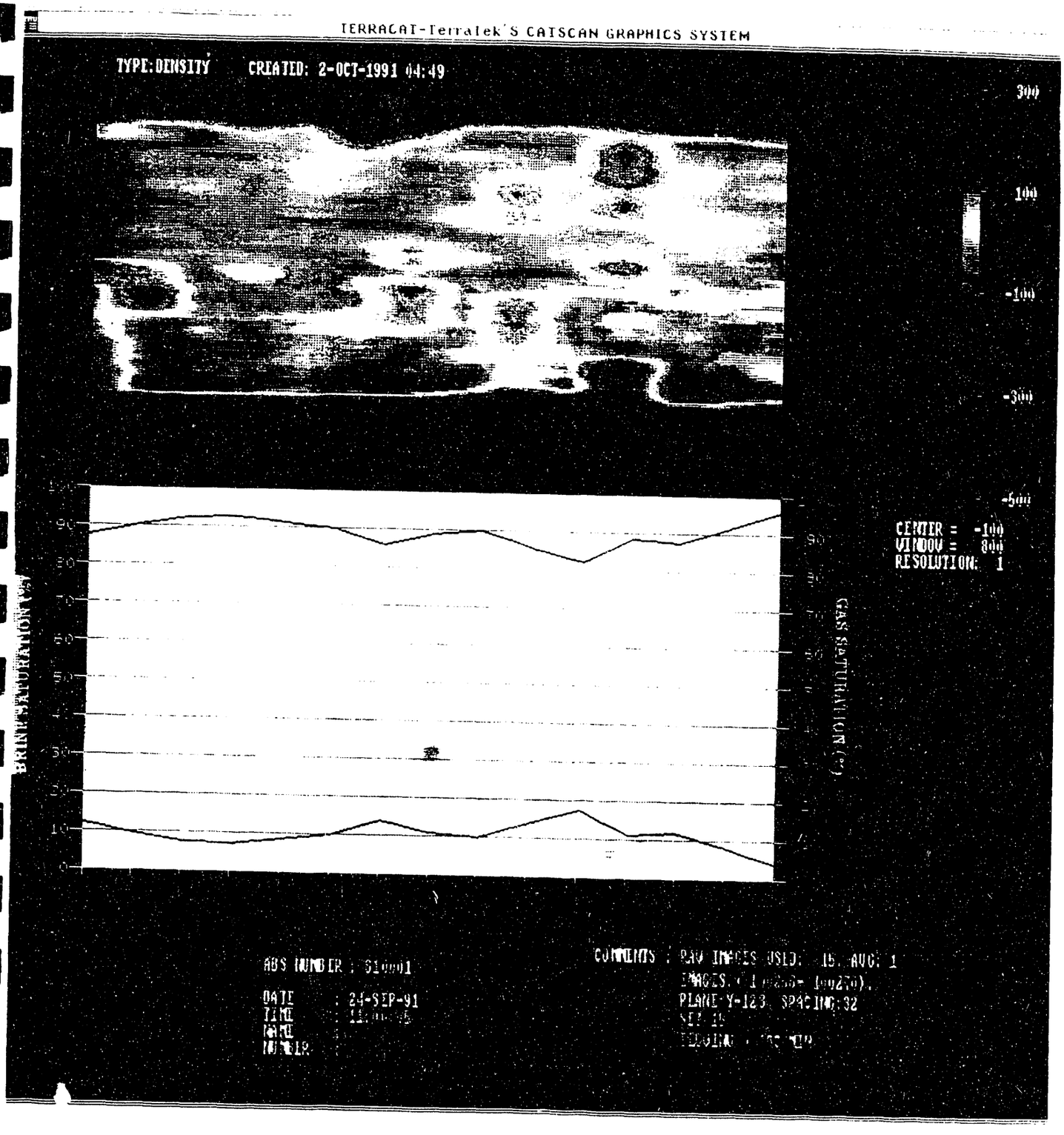
TERRACAT-Terratek'S CATSCAN GRAPHICS SYSTEM
TYPE:DENSITY
CREATED: 2-OCT-1991 04:49
300
100
-100
-300
-500
CENTER = -100
WINDOW = 800
RESOLUTION: 1
BRINE SATURATION (%)
GAS SATURATION (%)
ABS NUMBER : 810001
DATE : 24-SEP-91
COMMENTS : RAW IMAGES USED: 15. AVG: 1
PLANE-Y-123. SPACING:32

Figure 21.

Longitudinal Reconstruction
With Saturation Profile at
equilibrium at 0.4 cc/min.

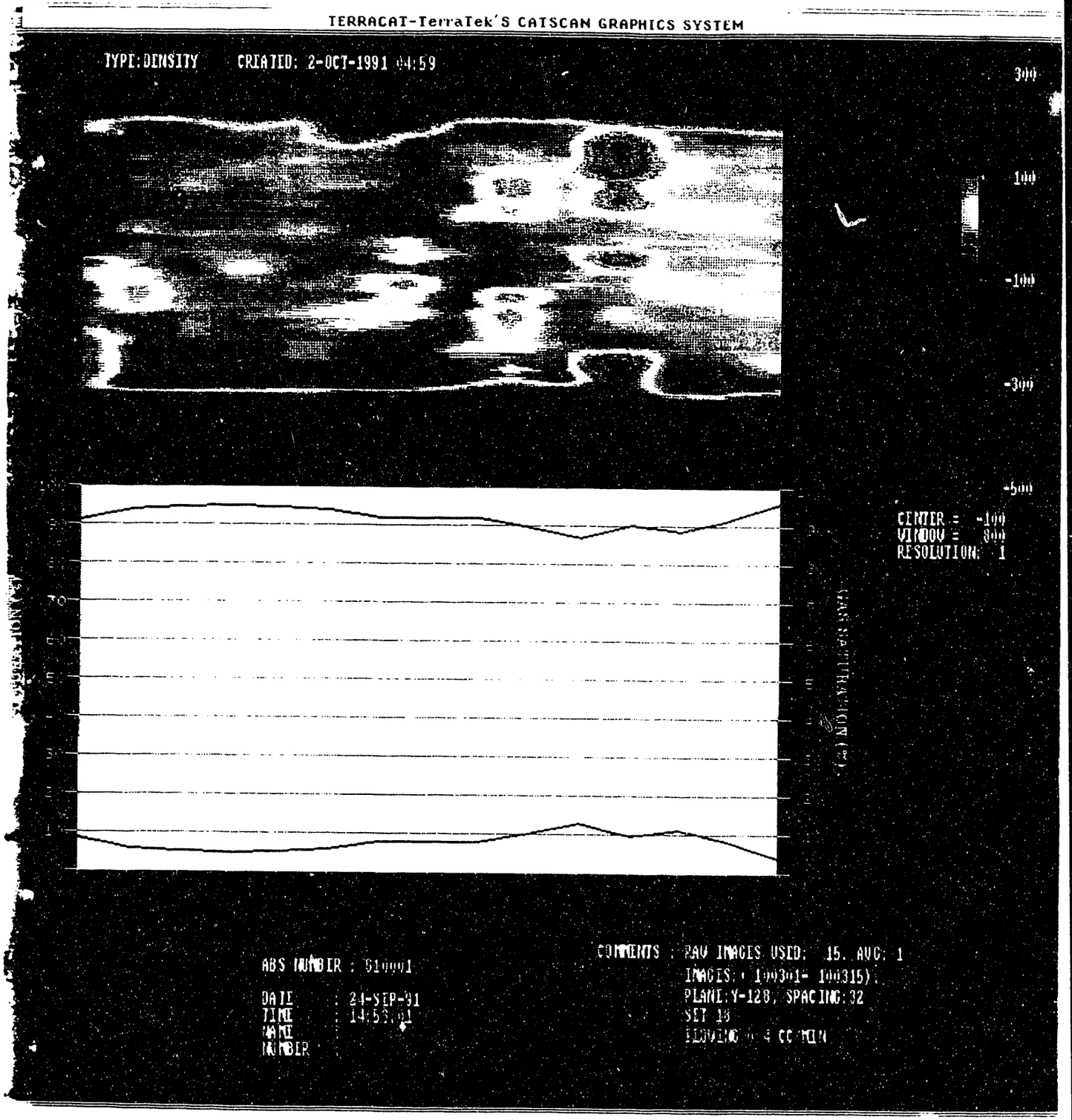

Figure 23

Longitudinal Reconstruction with Saturation Profile at equilibrium at 1.0 cc/min.

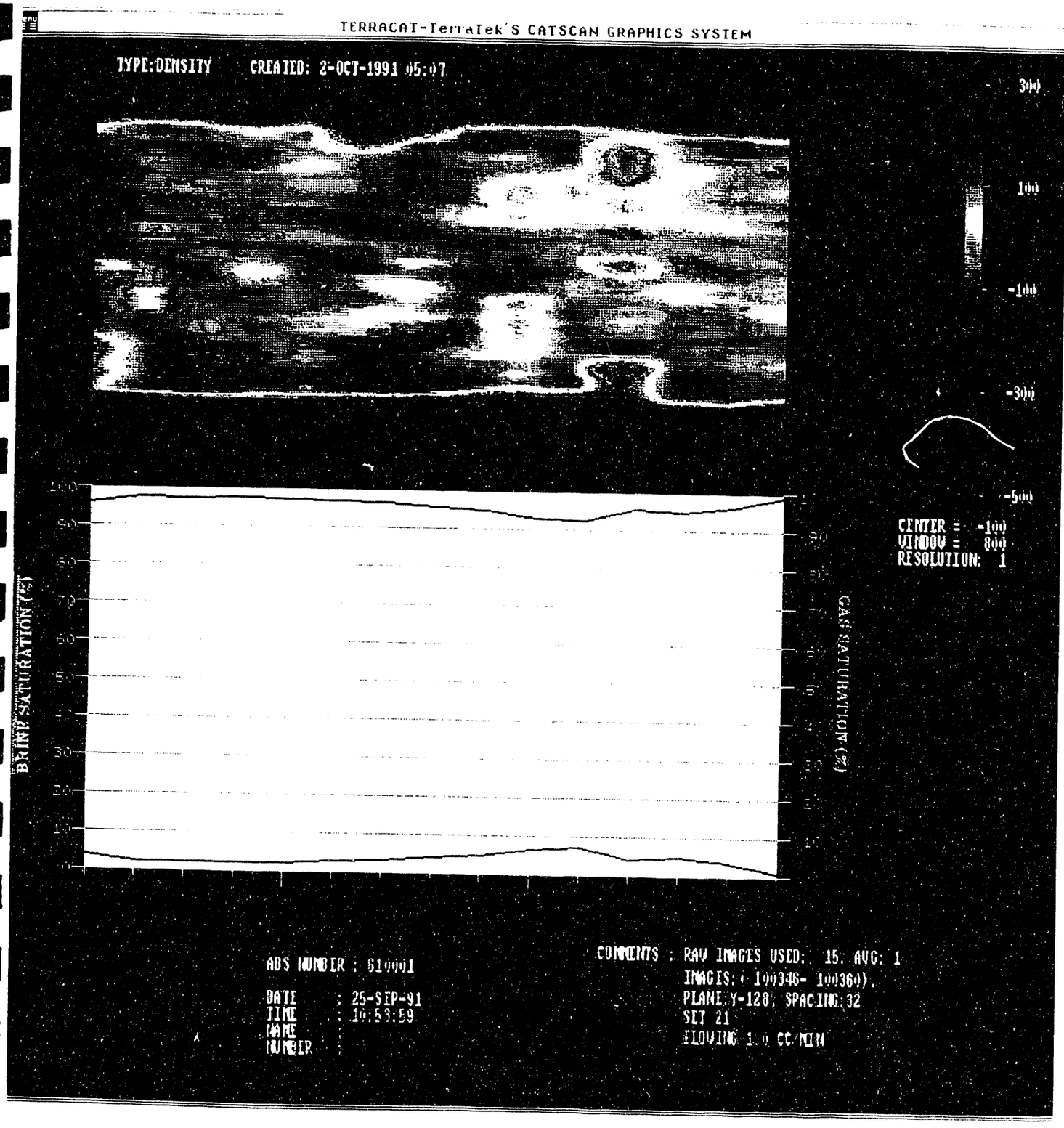

Figure 24

Longitudinal Reconstruction with Saturation Profile at Equilibrium at 2.0 cc/min.

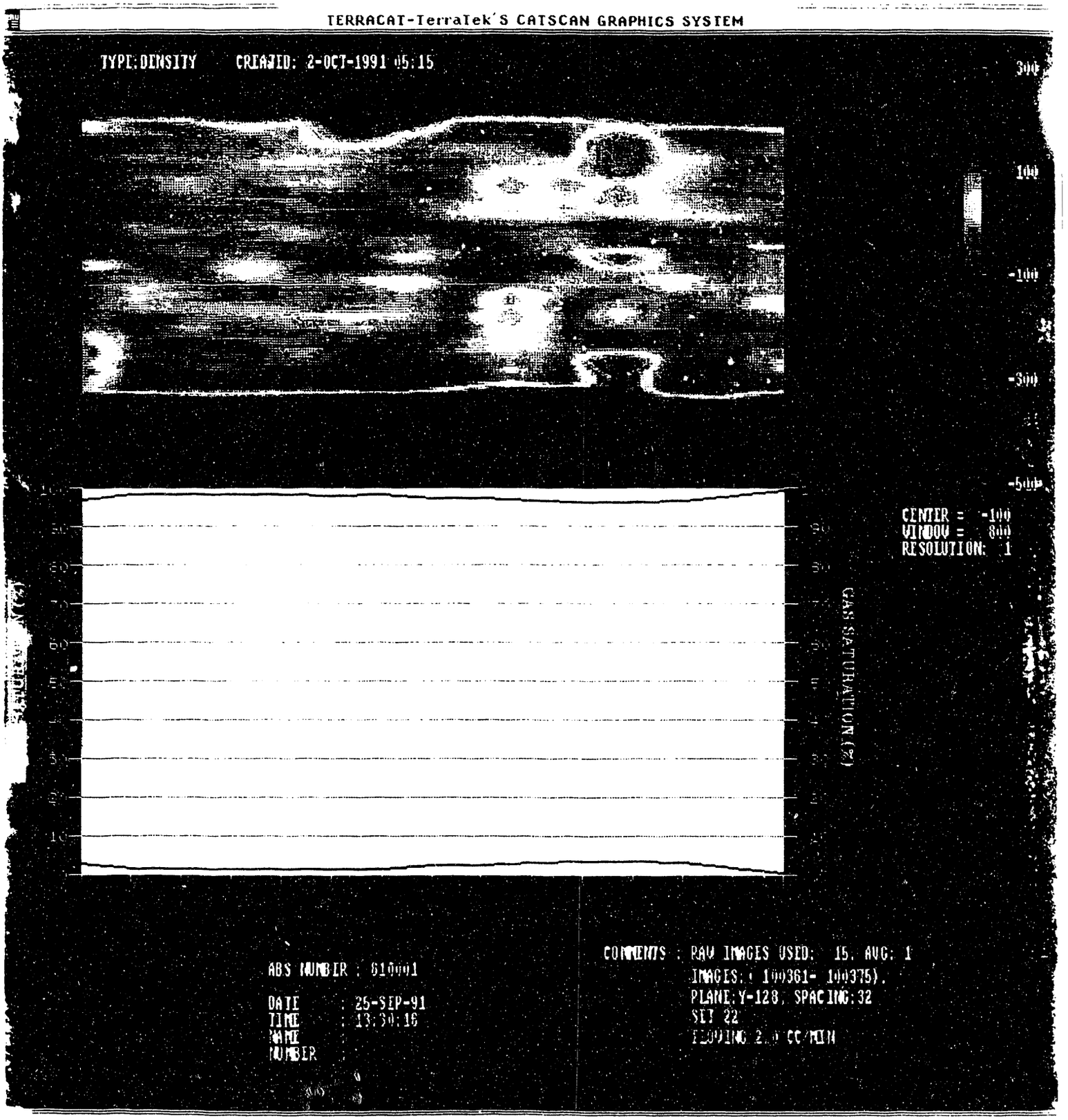

Longitudinal Reconstruction
with Saturation Profile at
equilibrium at 5.0 cc/min.

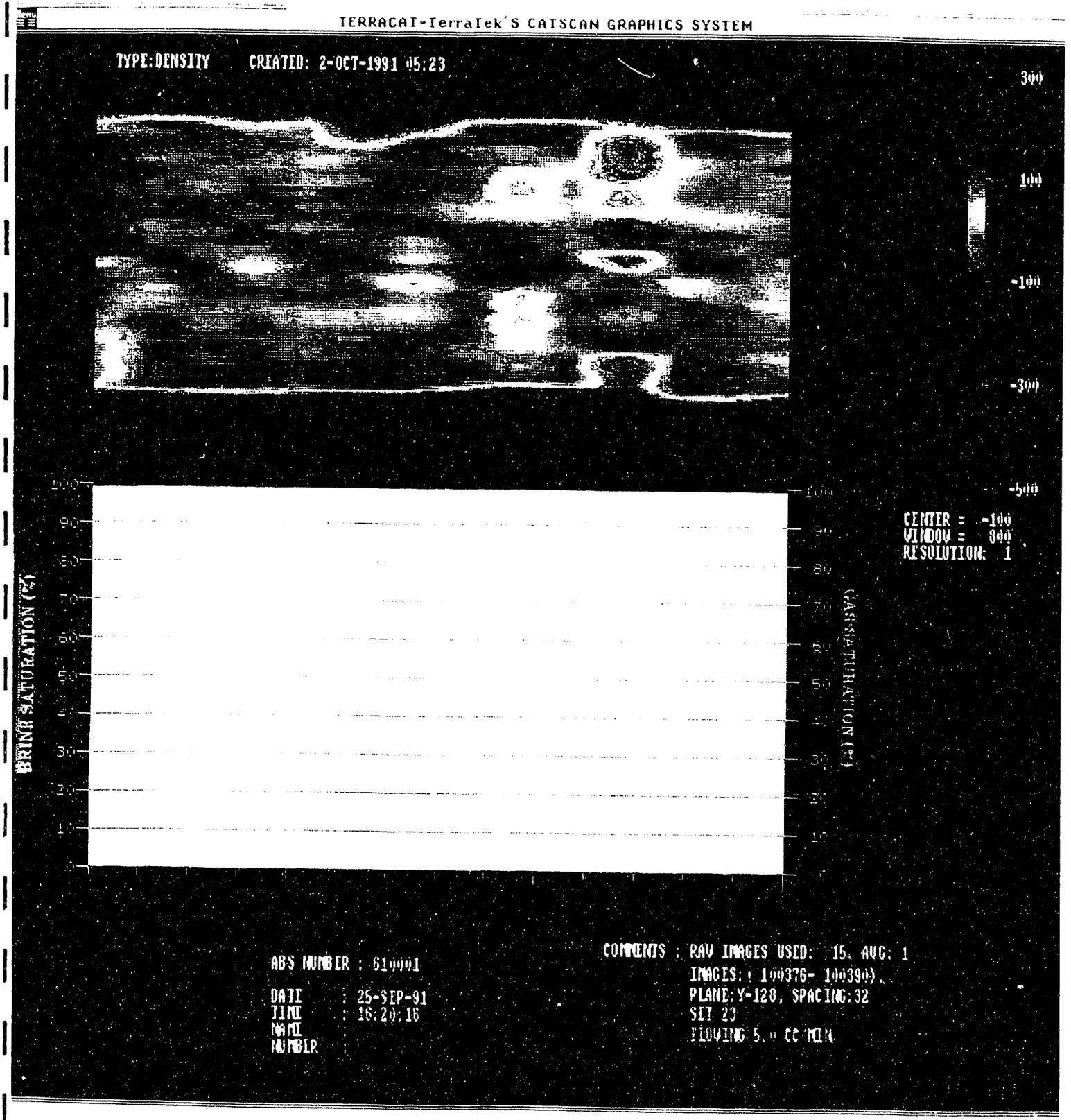

Longitudinal reconstructions are built from the cross sectional images. The color bar on the left-hand side of the reconstruction is used to interpret the degree of saturation of the sample. Colors are assigned in the same way and have the same meaning as for the cross sectional images. The CT number at the red end of the color bar is the upper limit for the chosen CT range and the number at the blue end of the bar is the lower limit for the range. Data elements with higher numbers than the upper limit are assigned the color red by default and those with numbers less than the lower limit are assigned black. The range of numbers from the upper value to the lower one is defined as the "window". The "center" of this window is the average value between the upper and lower limits. The window and center are chosen to give the most contrast in saturation for the sample.

3.2 Discussion

Figure 26 shows the cross sectional image of the 5th slice (i.e., 50 mm from the upstream end) at the end of each set for the 0.1 cc/min flow rate. After 1 hour, the fluid has been detected, as evident by the green-yellow color in the right half of the image. After 1.5 hours the degree of saturation has increased to 50% and the fluid distributed uniformly over the cross sectional area. The remaining images show the degree of saturation increasing but at a decreasing rate over the remaining time the 0.1 cc/min flow rate was maintained.

The images also indicate that the rock matrix was very effective at imbibing the water. As shown in Table 2, 7 hours were required to detect any measurable downstream discharge. The initial pore volume was estimated to be 95 cc. After 7 hours, approximately 42 cc of water was introduced into the sample or half the total pore volume, the measured discharge was 6% (2.6 cc).

A significant observation from these images is that the fracture did not influence the fluid flow or the imbibition characteristics. The flow path did not initiate at the fracture and flow radially through the sample. Instead, as already mentioned, the imbibition and flow were fairly uniform over the cross section. Overall, the CT scanning rate was greater than the imbibition rate. In addition, very little increase in saturation level was detected with the increase in flow rate. Figure 27 shows the cross sectional images at the 5th slice at the initial condition and at

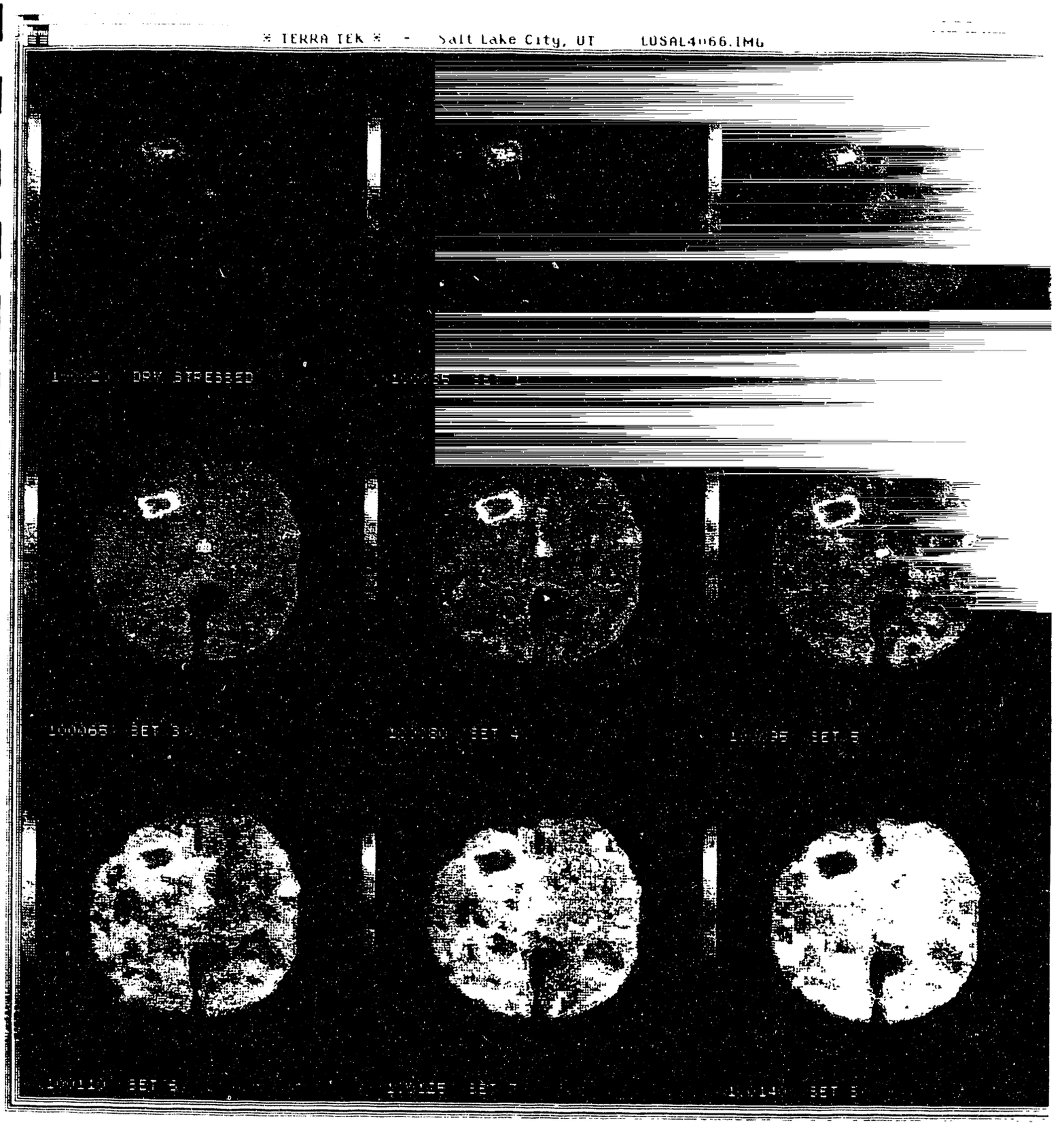
* TERRA TEK * - Salt Lake City, UT LOSAL4066.IMG
DRY STRESSED

Figure 26
(cont'd)

Cross Sectional Images of
Slice 5 at the End of Each
Data Set at 0.1 cc/min.

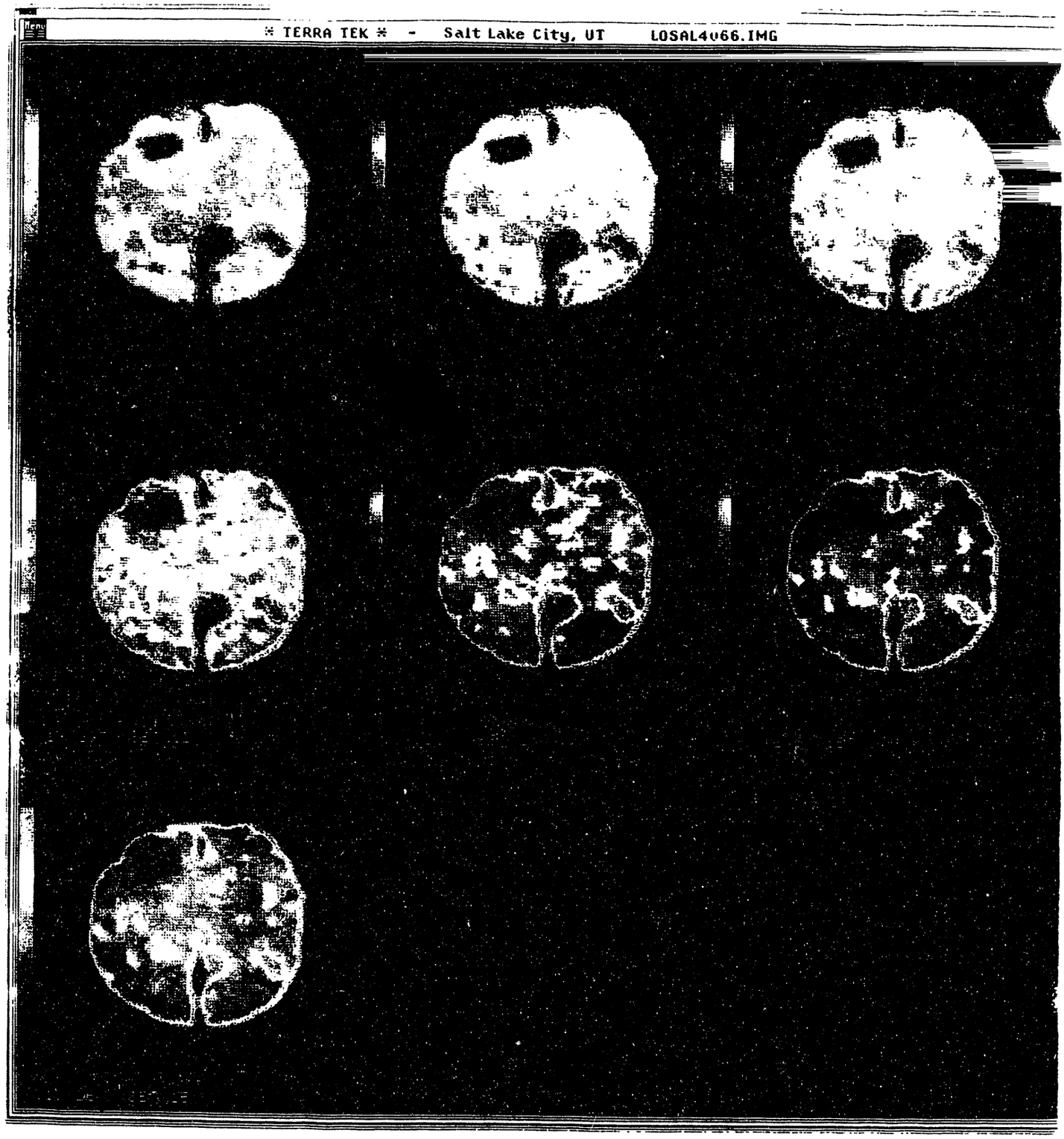

Table 2: Los Alamos Flow Test Data.

DATE	TIME	SCAN SET	FIRST IMAGE	LAST IMAGE	CUM FLOW	CUM PROD
23-Sep	07:00 PM	DRY-US	100001	100015	0.0	0.0
23-Sep	07:15 PM	DRY-S	100016	100030	0.0	0.0
@7:15 PM STARTED TO FLOW 0.1CC/MIN						
23-Sep	07:45 PM	1	100031	100045	3.0	0.0
23-Sep	08:15 PM	2	100046	100060	9.0	0.0
23-Sep	09:15 PM	3	100061	100075	15.0	0.0
23-Sep	10:15 PM	4	100076	100090	21.0	0.0
23-Sep	11:15 PM	5	100091	100105	27.0	0.0
24-Sep	12:15 AM	6	100106	100120	33.0	0.0
24-Sep	01:15 AM	7	100121	100135	39.0	0.0
24-Sep	02:15 AM	8	100136	100150	45.0	0.0
24-Sep	03:15 AM	9	100151	100165	51.0	0.0
24-Sep	04:15 AM	10	100166	100180	57.0	0.0
24-Sep	05:15 AM	11	100181	100195	63.0	0.0
24-Sep	06:15 AM	12	100196	100210	69.0	0.0
24-Sep	08:00 AM	13	100226	100240	76.5	0.0
24-Sep	09:40 AM	14	100241	100255	86.5	2.6
24-Sep	11:00 AM	15	100256	100270	94.5	10.9
24-Sep	12:00 PM	16	100271	100285	100.5	16.9
@12:30 PM STARTED TO FLOW 0.4CC/MIN						
24-Sep	01:30 PM	17	100286	100300	24.0	23.0
24-Sep	02:50 PM	18	100301	100315	54.0	53.0
@3:45 PM STARTED TO FLOW 1.0 CC/MIN						
24-Sep	04:30 PM	19	100316	100330	45.0	45.0
25-Sep	07:00 AM	20	100331	100345	OVERNIGHT	
25-Sep	11:00 AM	21	100346	100360	339.0	339.0
@11:30 AM STARTED TO FLOW 2.0 CC/MIN						
25-Sep	01:30 PM	22	100361	100375	240.0	240.0
@2:10 PM STARTED TO FLOW 5.0 CC/MIN						
25-Sep	04:20 PM	23	100376	100390	650.0	650.0

the end of each flow rate. The increase in flow rate increased the degree of saturation from 90% to 100%.

4.0 CONCLUSIONS

Computerized tomography has been used to provide a direct observation of flow characteristics in a fractured sample of Bandelier tuff. Hence, validating the usefulness of the technique to contribute to the understanding of the physical processes governing flow in fractured rock. The technique overcomes limitations in current laboratory studies of contaminant transport through the ability to observe contaminant distribution in real time under non-equilibrium conditions.

The study of contaminant transport is of ultimate concern to prevent their spread and to develop efficient remediation strategies. Contaminant transport mechanisms can involve mixed-phase flow through porous media, diffusion through the aqueous phase, and retardation by adsorption and absorption processes. Studies of contaminant transport can yield direct measurements of the diffusion rate of specific contaminants in specific rock types and under simulated in situ conditions. In addition, detailed observations can lead to an improved understanding of the mechanisms involved, and to better definitions of the most important rock and fluid properties controlling contaminant transport. Properly designed experiments can also be used to verify and improve contaminant transport models.

5.0 RECOMMENDATIONS

The following are recommendations for further study:

1. Investigate the flow and imbibition characteristics of identified contaminants using an actual contaminant or a simulant. Contaminants will be introduced at the upstream end and followed through the sample. Transport rate will now depend on diffusion as well as multi-phase flow parameters. The flow rate, overburden pressure and fluid pressure conditions will be the principle variables. The intent of the tests will be to provide transport rates for specific combinations of these variables and to correlate them with rock and fluid properties.

Figure [illegible]

Cross Sectional Images
of Slice [illegible]
End of Each Pile Face

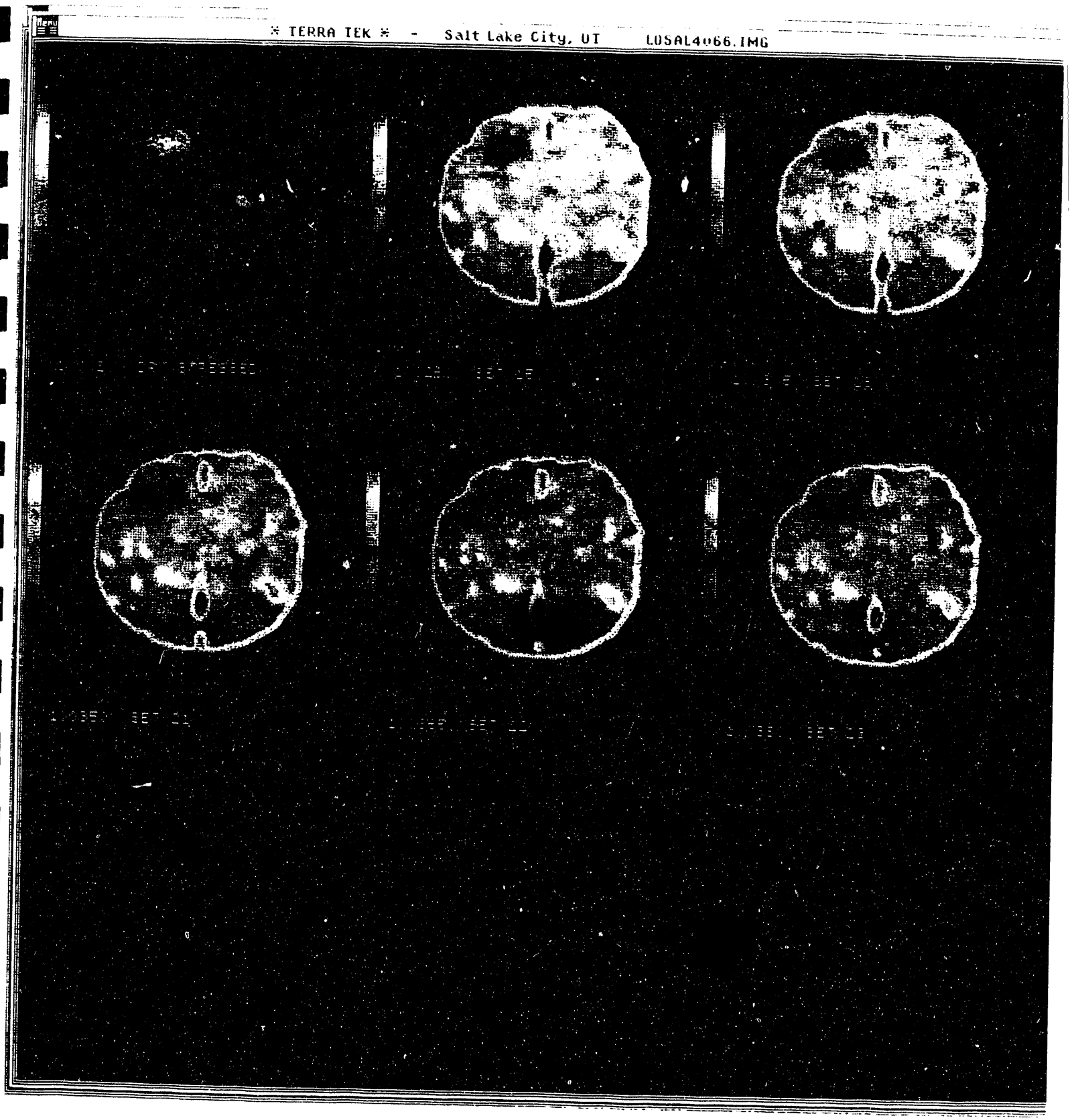

2. Investigate the flow and imbibition characteristics as a function of rock type and fracture parameters such as aperture, roughness, fill material, etc. The same concepts as outline in recommendation 1 would be followed.

3. Through small scale modeling construct a containment barrier and evaluate its effectiveness.

APPENDIX A: X-RAY COMPUTERIZED TOMOGRAPHY

A.1 CT Equipment

The CT scanner used at TerraTek is an Ohio Nuclear DeltaScan 100. It is a second generation medical CT imaging machine built in 1980 for use as a head scanner. Only minor hardware modifications were made to the scanner for use as a material imager.

The X-ray beam is collimated into three fan shaped beams which are attenuated as they pass through the sample. The width of the beam can be adjusted from 1 to 10 mm. The attenuated X-rays are measured by three detectors with measurements recorded every 3^0 in a 180° rotation. Each scan requires two minutes to complete.

The maximum diameter of a sample is limited to 304.8 mm (12 inches). However, with large samples resolution is decreased as the pixel array is fixed at 256 X 256. Also, the diameter must be adjusted according to the density of a sample for successful X-ray penetration.

A.2 Analysis

Computerized tomography (CT) is a non-destructive means of evaluating the internal structure of a material. X-ray CT technology is based on analysis of the attenuation of X-rays as they pass through a material. This attenuation is due to scattering and adsorption and is characterized by Beer's law:

$$I = I_o e^{-\alpha x}, \tag{A1}$$

where:

I_o = incident X-ray intensity,

I = attenuated X-ray intensity,

x = thickness of the material, and

α = linear attenuation coefficient.

The attenuation of the X-rays is dependant on photoelectric adsorption and Compton scattering. Photoelectric adsorption is dependent on the electron density or the effective atomic number of the material and is a predominant term at X-ray energies below 100 keV. Compton scattering is dependent on the density of the material and becomes a more predominant term at energy levels above 100 keV. Therefore, the attenuation coefficient of a material is a function of the density and effective atomic number of the material and the energy level of the X-ray.

The following relationship gives the dependence of the linear attenuation coefficient in terms of mass density, effective atomic number and X-ray energy level:

$$\rho\left(a+\frac{bZ^{3.8}}{E^{3.2}}\right) \qquad \text{(A2)}$$

where:

ρ = mass density of the material,

Z = effective atomic number,

E = X-ray energy level,

a = Klein-Nishina coefficient, and

b = a constant.

At high energy levels, and for materials with similar chemical composition, differences in the effective atomic number are small. Differences in attenuation are therefore due primarily to differences in mass density. Similarly, any changes in attenuation, for example due to stress, must also reflect a change in mass density. By calibrating the equipment against a material of known density (e.g., fused silica for work with rock), attenuation data can be converted to density data with an accuracy of approximately 0.02 gm/cm^3.

CT technology measures the attenuation coefficient in small volume elements of the sample. When a test sample is inserted in the scanner, an X-ray source and detector are passed in parallel planes past the sample (called a traverse). Figure A.1 illustrates this operation. The tube and detector are then rotated through a specified number of degrees and another traverse occurs. This is repeated through a 180-degree rotation. With these data, a cross-sectional image of the test sample can be generated by dividing the sample up into small discrete elements or pixels and solving a set of linear equations. The linear attenuation coefficient for each element can be determined through reconstruction algorithms.

As shown in Figure A.2, a typical pixel array is 256 x 256 in size. The thickness of the collimated X-ray beam can be adjusted from 1 mm to 10 mm depending on the resolution required. The slice thickness then determines the volume of material (voxel) for which linear attenuation coefficients are calculated. Also, by taking multiple slices of a test sample, three-

dimensional arrays of data are collected and profiled such that reconstruction of the image in any two dimensional plane can be provided.

A.3 Cross-Sectional Images

Cross-sectional images are the illustrations depicting an individual CT scan. Each cross-sectional image is made up of a 256 x 256 array of data. This data array is composed of CT numbers collected from the scanner. These CT numbers are defined as normalized attenuation coefficients for the material being scanned.

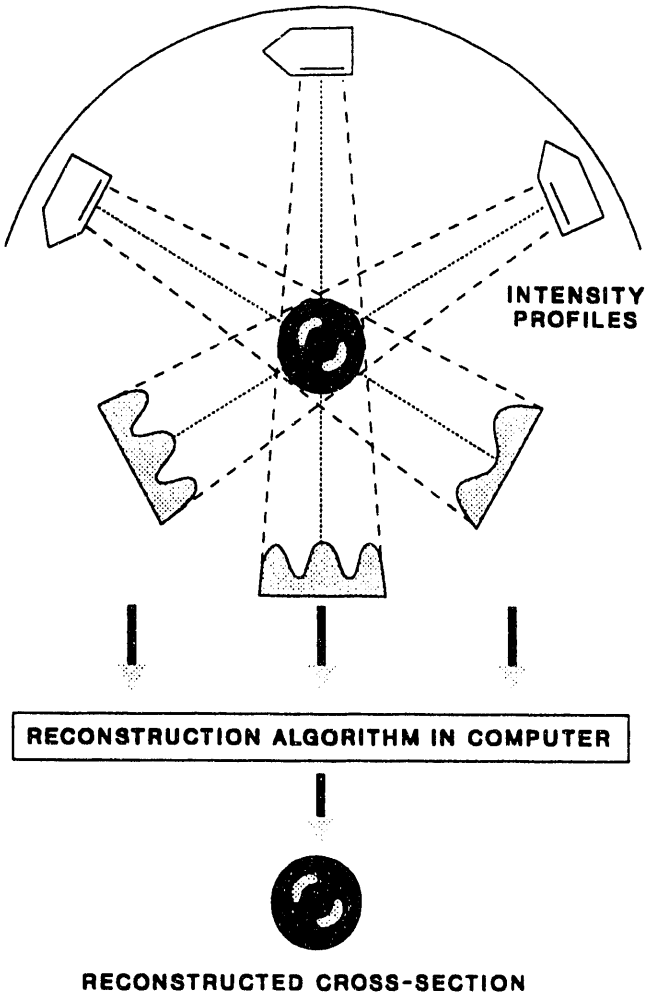

Figure A.1: Computerized Tomography Schematic.

Cross-sectional images are useful for a variety of reasons. A visual picture of the sample shows the presence of fractures, filled fractures, vugs, and mineral inclusions. Fractures as small as 0.25 mm can be detected. Further studies can be performed on specific regions of interest based on the information obtained from the cross-sectional pictures. Also, broken or crushed sections of core can be identified before the sample is removed from its packaging, aluminum casing, or rubber sleeves. This form of documentation complements more conventional forms of core records such as photographs or slabbing.

A.4 Longitudinal Reconstructions

Longitudinal reconstructions are built from a series of cross-sectional images. They are created by averaging 6 contiguous rows or columns of data elements for each cross section in the series. The rows or columns can be in either the x or y direction depending upon the plane of interest in the sample. The reconstructed image is made by displaying the averaged data and

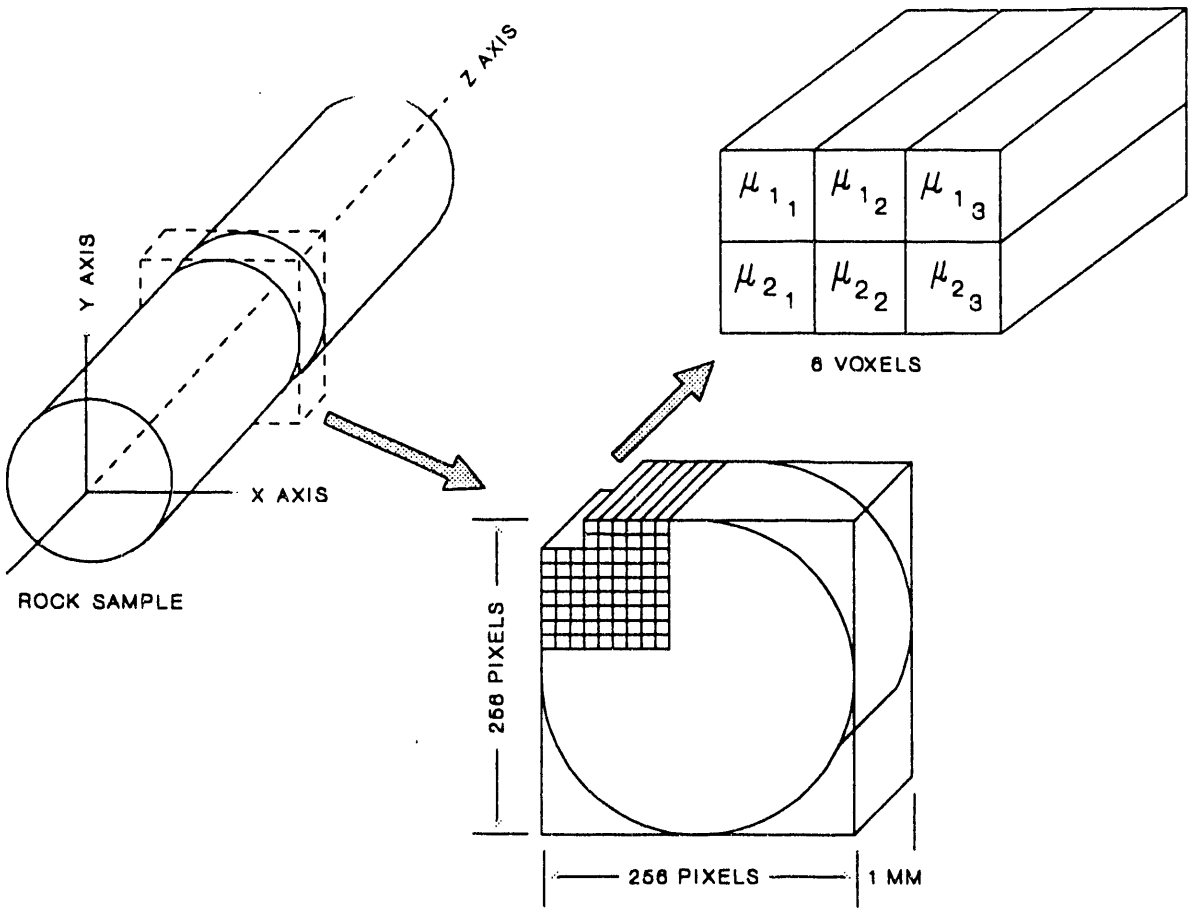

Figure A.2: Schematic of CT-Scanner Terminology.

interpolating between scans to complete the visualization. The resultant image represents the core as it would appear if it were slabbed through the x or y plane as defined above.

Longitudinal reconstructions show a degree of detail relative to the scanning frequency of the sample. If the scanning frequency is continuous, a complete lithology of the sample is obtained. As the scanning frequency is decreased, the reconstruction appears "smeared" due to the reduced number of real data points and the increased number of interpolated points. A higher scanning frequency is needed when a more detailed lithology is required.

END

DATE FILMED

5/5/93